NATIONAL ADVISORY COMMITTEE FOR AERONAUTICS

TECHNICAL NOTE

No. 1540

THE EFFECT OF TIP MODIFICATION AND THERMAL DE-ICING AIR FLOW ON PROPELLER PERFORMANCE AS DETERMINED FROM WIND-TUNNEL TESTS

By W. H. Gray and R. E. Davidson

Langley Memorial Aeronautical Laboratory
Langley Field, Va.

Washington

February 1948

ERRATA AND ADDENDUM

NACA TN No. 1540

THE EFFECT OF TIP MODIFICATION AND THERMAL DE-ICING AIR FLOW ON PROPELLER PERFORMANCE AS DETERMINED FROM WIND-TUNNEL TESTS

By W. H. Gray and R. E. Davidson

February 1948

In the second paragraph under the heading "Torque of Graphite Seals," page 12, the values for efficiency loss and net efficiency are in error. The paragraph should read: "For the peak-efficiency condition at a blade angle of 40°, the rotational drag when charged to the propeller resulted in an additional 0.8 percent decrease in efficiency, or a net efficiency of 0.899. The losses from this source are about three-fourths of those entailed by the introduction of tip nozzles and internal air flow."

In regard to the discussion of the torque of graphite seals, the manufacturer advises that much smaller values of friction horsepower have been obtained by employing graphite seals sliding in chromium-plated steel parts. The materials furnished for the NACA tests, however, were graphite seals sliding in duralumin parts, which combination showed considerable wear as a result of less than 55 hours of running time.

For the above reasons, the last paragraph of the Summary, page 1, and Conclusion 6, page 13, are invalid and should be deleted.

NATIONAL ADVISORY COMMITTEE FOR AERONAUTICS

TECHNICAL NOTE NO. 1540

THE EFFECT OF TIP MODIFICATION AND THERMAL DE-ICING AIR FLOW ON PROPELLER PERFORMANCE AS DETERMINED FROM WIND-TUNNEL TESTS

By W. H. Gray and R. E. Davidson

SUMMARY

Results are presented of the effects on propeller efficiency of thermal de-icing of airplane propellers by use of internal flow through hollow blades. Wind-tunnel tests were made of a propeller with blades embodying tip orifices. Provision was made for heating the internal flow to about 285° F.

The flow through the tip nozzles of good external design but with poor internal ducting caused peak efficiency losses of little more than 1 percent. When heat was added no additional change of efficiency was found. Computation of the efficiency losses by a theoretical method resulted in a fair check with the values experimentally obtained.

Bench tests employing smoke indicated that the internal ducting of the blade should be faired to the tip nozzle. A minor addition to the internal ducting leading to the nozzle improved the flow considerably.

The torque of the spinner-juncture seals necessary to this design was excessive, and large efficiency losses resulted when this torque was charged to the propeller.

INTRODUCTION

Consideration of the propeller-blade icing problem over a period of many years has indicated several possible solutions. One of the most promising solutions, and the one herein described, employs the passage of heated air through hollow blades, the flow emitting from a nozzle near the blade tip. In the application of the system to flight conditions, it is intended that the flow of air shall be continuous, that heat should be applied only during actual icing conditions. Numerous flight tests, as well as several wind-tunnel investigations, have demonstrated that this method is both structurally and aerodynamically feasible. In one

case, however, rather large discrepancies existed between the aerodynamic loss entailed by the use of such a system as evaluated in wind-tunnel and flight tests of similar blades.

A method of evaluation of efficiency losses occasioned by the presence of the tip nozzle has been presented in references 1 and 2, and the results of wind-tunnel tests of blades employing tip nozzles have been evaluated by means of this method. Unfortunately, the nozzles tested proved unnecessarily large and were of aerodynamically poor design. A satisfactory blade-tip-nozzle design, that is, one which has the least detrimental effect on section drag and lift, has since been developed.

The present investigation was made to determine conclusively the actual losses, as well as the accuracy of the analytical method, in conjunction with tip nozzles of the best size and shape. Heat was added to the internal flow to simulate operating conditions as nearly as possible, and all necessary ducting for the internal flow was constructed in a manner typical of a contemporary installation.

APPARATUS

Dynamometer.- The NACA 2000-horsepower propeller dynamometer of the Langley 16-foot high-speed tunnel, the essential details of which are described in reference 3, was used for these tests. Some modifications of spinner fairing lines were necessary, however, since the spinner used was 2 inches smaller in diameter than the standard spinner described in reference 3. Minor additional alterations were necessary to provide for the induction, measurement, and heating of the internal air (figs. 1 and 2).

Internal-flow system.- A protuberance on the existing fixed fairing covered all the metering and heating units except the venturi entrance, at which point air was induced for the internal flow. Because the internal-flow inlet opening was located in the propeller slipstream, the total pressure was subject to change with changing propeller operating conditions, and both total-pressure and static-pressure measurements in the venturi were required for each measurement of mass flow.

The throttle in the after end of the venturi was installed to find the effect of variation of mass flow on the propeller aerodynamic characteristics. As is explained subsequently herein, certain factors limited the use of the throttle in obtaining design values of mass flow.

An electric heater was installed downstream from the venturi in the duct system. A rheostat in the field of a motor generator set permitted accurate control of the voltage across the heater terminals

and, therefore, allowed output temperatures to be controlled readily within $\pm 2\frac{1}{2}^{\circ}$. For the mass flows investigated, the heater was capable of supplying air at 500° F. A thermocouple measured air temperatures from the heater. The induction system from the venturi to the annular manifold was attached to a floating component of the dynamometer. All forces resulting from the induction of the de-icing air were, therefore, automatically included in the measurement of propeller thrust. The external drag values of the induction system were reduced as much as practicable by enclosing all but the venturi entrance within a fixed fairing. Leakage around the venturi entrance was reduced by a rubber seal.

The annular manifold received the de-icing air ducted from the venturi and heater. Large holes on the inner face of this manifold allowed the air to pass across the narrow gap to the rotating spinner bulkhead. The bulkhead was cut out behind each blade shank to provide an air passage to the blade-shank ducts. The path of the air from these ducts was through shank holes to the blade itself and thence to the tip exit nozzle. Between the shank and the tip exit nozzle the flow was confined to the leading-edge half of the blade by a partition within the blade.

Segmented graphite seals were provided to reduce leakage to an allowable minimum at the blade shanks and at the spinner periphery, the two points in the internal system where there was relative motion between parts.

Blades.- A two-blade propeller with blades of modified Curtiss design No. 528 was employed in the tests. The blades, as received, were furnished with a spanwise Fiberglas partition riveted to the inner faces of the upper and lower surfaces but no tip orifices had been cut. Following the no-flow (no-tip-nozzle) tests, the tip nozzles were cut and the tests were continued with internal flow.

Visual examination indicated slight distortion of the blade sections at the points at which the partition was riveted. Since, however, the tests are for comparitive purposes only, the effects of such distortion may be considered the same for each of the configurations tested. Absolute values of the aerodynamic characteristics may be somewhat in error if the uncut blades are considered to be representative Curtiss 528 blades.

Standard Curtiss 528 blades embody NACA 16-series sections throughout, and the blade-form curves are presented in figure 3.

Two roughly elliptical holes, each of area 0.409 square inch, had been cut in each blade shank at locations considered to be least detrimental structurally. These holes were larger than necessary and permitted more internal mass flow than specified by the design conditions.

In the base of each blade shank, a rubber compound had been poured to seal the shank at the end of the partition. Internal flow was thus prevented from entering any part of the blade except that between the partition and the leading edge.

Tip orifice.- Several series of tests have been undertaken to improve the design of the blade-tip nozzle. In these unpublished tests, half-scale models of the tip of the propeller blade with two tip nozzles were mounted in a small wind tunnel. Lift and drag changes resulting from the addition of the nozzles were recorded at varying angles of attack. The nozzle used in the present thermal de-icing tests was similar to the better of the two nozzles used, except that in the present case no fairing was used between the radial partition and the orifice. The radial partition located at the 50-percent-chord station of the blade sections ended within 3.48 inches of the tip; thus the internal de-icing flow is permitted to turn from a spanwise to a chordwise direction to emit from the tip orifice (figs. 4 and 5). The orifice with its geometric center located 2.11 inches from the tip of the blade had a projected area normal to the chord of 0.3904 square inch on one blade and 0.3926 square inch on the other, making a total area of 0.00544 square foot. Unlike the orifices employed in the previous wind-tunnel investigation (reference 1), there was no deformation of the blade upper surface; the orifice consisted merely of a smooth hole cut in the upper surface near the blade tip.

TESTS

Scope.- The propeller was investigated in two different blade configurations, first as received and then as a propeller with open tip nozzles and with internal air flow both heated and cold. In both configurations the propeller was tested over a range of blade angle and a combination of forward speeds and rotational speeds which simulated operation of the propeller in appropriate flight applications. At the two highest blade angles tested, power requirements necessitated that the rotational speeds be somewhat lower than desired.

The blade angles tested covered the range at the 42-inch radius from 20° to 55° in 5° increments. The electric hub furnished was employed to change and lock the blade angles. The initial blade settings for the uncut blades resulted in some slippage because of the tendency of the blades to return to low pitch. It is certain that the slippage occurred immediately at the start of the run and that the blade angles remained constant at those values marked in figures 6 to 8, which in each case are the angles measured at the completion of the run. Improved technique resulted in no blade-angle slippage for the tests with internal flow. Tests of cold and heated internal flow at each blade angle were made consecutively, thus insuring identical blade-angle settings.

Mass flow.- It was not feasible to obtain the desired values of design mass flow. The mass flow could have been corrected by operation of the venturi throttle in an almost closed position; however, under the resulting conditions the differential pressure across the spinner-periphery seal would have exceeded 15 inches of water. This pressure differential was selected as a reasonable value to which the pressure should be limited in order to enable the completion of the test program without failure of, or excessive wear on, the graphite seals. A throttle opening greater than desired was selected, therefore, which permitted somewhat greater than design mass flows.

Heat.- The quantity of heat leaving the electric heater was controlled by the regulation of the temperature output within $\pm 2\frac{1}{2}^\circ$ of 285° F as indicated by the heater exit thermocouple. A temperature drop of 35° between the measuring thermocouple and the blade shanks was estimated. The blade shanks could not be operated at temperatures exceeding 250° F because of the presence therein of a rubber sealing compound susceptible to failure at elevated temperatures under the action of centrifugal force. No satisfactory substitute for the compound was immediately available.

Bench tests.- A few bench tests were carried out following the wind-tunnel tests. The blade tip, including the nozzle, was surrounded with a low-pressure chamber; and, by suitable instrumentation of the pressure chamber, blade tip nozzle, and venturi, the pressure drop through the system and the density of air at the nozzle were determined. Although the blade tip was fixed in the low-pressure chamber, the effect of a blade-angle change on the internal air flow at the blade shanks could be obtained by rotation of the hub around the blade shanks as its axis. In additional tests, smoke was blown through the blade in order to determine the nature of the flow at the tip nozzle.

REDUCTION OF DATA

Symbols.- The test results, corrected for tunnel-wall interference, are presented in the form of the usual thrust and power coefficients and propeller efficiency. The symbols and definitions used are as follows:

A_V	cross-sectional area of metering venturi (0.0096 sq ft)
A_N	geometric total tip-nozzle area (0.00544 sq ft)
A_N'	effective total tip-nozzle area, square feet
b	blade chord, feet
c_l	section design lift coefficient

C_{D_N} nozzle drag coefficient

C_P power coefficient $(P/\rho n^3 D^5)$

C_T thrust coefficient $(T/\rho n^2 D^4)$

D propeller diameter (10.19 ft)

g acceleration due to gravity (32.2 ft/sec^2)

h blade section maximum thickness, feet

J advance ratio (V/nD)

M Mach number

M_t helical tip Mach number

m mass-flow rate of de-icing air, slugs per second

m_c coefficient of mass flow of de-icing air $(m/\rho A_N nD)$

n propeller rotational speed, revolutions per second

N propeller rotational speed, revolutions per minute

P power absorbed by propeller, foot-pounds per second

Δp_f total pressure loss across internal flow system, pounds per square foot

p_V static pressure in metering venturi, pounds per square foot

Δp_V pressure difference in metering venturi, pounds per square foot $\left(\Delta p_f - p_V\right)$

q_N dynamic pressure at nozzle, pounds per square foot $\left(\frac{1}{2} \rho_N V_N^2\right)$

R universal gas constant (53.34 ft-lb/lb $^\circ$F for air)

T propeller thrust, pounds

t_V venturi stagnation air temperature, $^\circ$F absolute

V free-stream airspeed, feet per second

V_N velocity of air leaving nozzle, feet per second

x fraction of propeller tip radius

β blade angle, degrees

ϵ nozzle effectiveness; cosine of total included angle between path of flow from nozzle and helical path of nozzle

η propeller efficiency $\left(\frac{C_T J}{C_P}\right)$

γ ratio of specific heats for air (1.40)

ρ mass density of air in free stream, slugs per cubic foot

ρ_N mass density of internal flow at nozzle, slugs per cubic foot

Reduction of force data.- The reduction of force data was accomplished as described in detail in reference 1. A few pertinent points are reiterated here for clarity.

The values of thrust coefficient presented are based on corrected values of shaft tension caused by the propeller forces only. Corrections to data have been applied to cancel the effects of spinner forces and the drag forces on the venturi entrance extending into the air stream. Glauert's correction for wind-tunnel wall interference has been applied to the velocity measurements; all velocity data presented are for equivalent free-stream airspeed.

Reduction of mass-flow data.- Because of the location of the metering venturi behind the propeller disk, it was necessary to measure static and total venturi throat pressures as well as temperature. The form of the compressible-flow equation used to compute mass flows was

$$m = A_V \sqrt{\frac{2\gamma}{(\gamma - 1)gR}} \frac{p_V}{\sqrt{t_V}} \sqrt{\left(1 + \frac{\Delta p_V}{p_V}\right)^{\frac{\gamma-1}{\gamma}}} \sqrt{\left(1 + \frac{\Delta p_V}{p_V}\right)^{\frac{\gamma-1}{\gamma}} - 1}$$

A coefficient of mass flow defined in reference 2 to be consistent with other propeller coefficients is given as follows:

$$m_c = \frac{m}{\rho A_N n D}$$

RESULTS

Force Data

General aerodynamic characteristics.- Conventional propeller characteristics of the uncut blades (fig. 6) indicated normal results and normal efficiencies for a propeller with blades having such a plan form, thickness, and blade section. For the relatively low Mach numbers at which the tests were run, there appeared to be no serious effect from the deformation of the blade sections at the internal-partition attachment points. Figures 7 and 8 present characteristics of the blades with cold and with heated internal flow, respectively. Several repeat tests at the higher blade angles indicated an ability to repeat data within 1 percent. Repeat tests of doubtful data at very low and very high blade angles were precluded, however, because of failure of the rivets supporting the blade partition.

It will be noted that the smooth efficiency curves in figure 9 are the envelopes of the lower blade-angle efficiency curves in figures 6(c), 7(c), and 8(c) but are not tangent to the 55° blade-angle curves. The $1\frac{1}{2}$ percent better efficiency at this blade angle may be attributed in part to the lower rotational speed value of 960 rpm. This rotational speed resulted in a tip Mach number of only 0.61 at $J = 2.9$ compared with values of M_t of 0.715 at 1140 rpm and roughly 0.865 at 1350 rpm. (See fig. 10.)

Effect of internal flow.- The difference between the efficiency of a propeller with uncut blades and the same one with tip orifices and internal flow represents the net loss in efficiency caused by these modifications. Internal flow is specified because it is intended that the propeller will always be operated with internal flow. The propeller envelope curves (fig. 9) show losses up to 1 percent for the blades with cold internal flow, except at very low values of J, where a crossover of the envelope curves occurs.

Effects of heat.- The effects on propeller efficiency of adding heat to the internal flow for temperatures of the order of 350° F at which thermal anti-icing systems operate can be shown to be negligible by computation using the methods of reference 2. This method of computation neglects any effects of heat transfer on the external flow, but such effects would be expected to be very small at the low heating rates involved. Although the temperature used in the present tests (250° F) was somewhat lower than would be anticipated in practice, the lack of any measurable effects of heating is in agreement with expectations. Differences in efficiency, as small as those indicated in figure 9, between cold and heated flow are less than the limit of accuracy of these tests.

Effect of internal flow for one blade angle.- Small and inconclusive differences may be noted in figure 11 for values of J other than for peak efficiency. Apparently, within the accuracy of the tests, 1 percent may be considered the average percentage by which the addition of this particular tip nozzle with internal flow will affect the efficiency of the Curtiss 528 blade. Since the mass flow was somewhat larger than the design value, the characteristics would be expected to vary according to the efficiency of the tip nozzle.

Internal Flow

General flow characteristics.- It was believed that the use of a tip-nozzle area measured in a plane perpendicular to the chord of a blade section at the nozzle would be incorrect in any analysis of the present unrevised nozzle. In conjunction with bench-test studies of the internal flow, therefore, smoke studies were made of the flow from the blade tip. Figures 12(a) and 12(b) illustrate the poor flow obtained. It may be seen in figure 12(a) that the flow emerged from the nozzle in a direction other than optimum, which should coincide with the extended chord of a blade section at the nozzle. The angularity of the flow to the chord line was determined to be 31°, which measurement indicated that the nozzle area was very nearly that determined by a plane intersecting the blade and passing through the upper surface lip of the nozzle perpendicular to the lower surface of the blade. In addition to this angularity which affects the value of A_N', part of the flow turns upward at an angle averaging approximately 30° (fig. 12(b)). The cosine of the total angle between an ideal chordwise flow at the tip nozzle and the average actual flow has been taken as the nozzle effectiveness ϵ as defined in reference 2.

The nearly perfect flow conditions indicated in figure 6, page 78, of reference 4 have been sacrificed by a combination of construction details. Undoubtedly the flow at the tip nozzle could be improved by ducting the flow directly to the tip nozzle. In order to demonstrate the latter point with the present nozzle, internal ducting was added as shown in figure 13.

The photographs of flow conditions obtained with the internal fairing lines showed essentially chordwise flow at blade sections through the nozzle (fig. 14(a)) with very little turning upward of the flow (fig. 14(b)). Most of the improvement in flow resulted from the fairing between the blade partition and the nozzle rather than the fairing between the bond line and the nozzle.

Evidently very little improvement in the tip-nozzle flow may be obtained by making the upper-surface nozzle lip parallel to the blade axis or by removing the bulbous section of the lower surface after the nozzle (section A-A, fig. 5).

Computation of combined losses.- Through the use of a mass-flow coefficient m_c, computation of the combined losses sustained by the system with nozzle and internal flow may be made. The actual values of m_c have been faired in figures 15(a) and 15(b). The mass-flow coefficient was reduced when heat was added.

The same trend that was indicated in reference 1 for the mass-flow coefficient to increase with increase in propeller-advance ratio is apparent. In contrast to the previous tests, however, there was very little change in mass-flow coefficient with rotational speed. Another point to be noted was that for a given rotational speed a faired curve tangent to the curves of m_c against J for each blade angle could not be fitted by the theoretical hyperbola having constant values of $\Delta p_f/q_N$ and ρ_N/ρ as in reference 1. Values of $\Delta p_f/q_N$ and reciprocal values of ρ_N/ρ obtained from an analysis of the mass-flow measurements are given in table I.

Values of $\Delta p_f/q_N$ and reciprocal values of ρ_N/ρ obtained in bench tests are also presented in table I. The latter values represent twice as much flow through a single blade for a given mass flow as would normally be experienced since only one blade was used in the bench tests. The setup was not flexible enough to permit a range of mass-flow measurements, but a rough check indicated that the greater part of the pressure drop occurred within the blade proper.

The blade angle in these bench tests could be changed by rotating the hub around the shanks as an axis. The effect of a blade-angle change was to alter by a slight amount the internal-flow path to the shank holes. No variation of $\Delta p_f/q_N$ for different blade angles could be found. The variation of $\Delta p_f/q_N$ and ρ_N/ρ with blade angle for a constant rotational speed, as well as the small change in mass-flow coefficient with rotational speed, was therefore believed to be caused by leakage in the system that gave rise to errors in mass-flow measurement. The method employed in reference 2 - that of inducting the air directly at the propeller hub and passing it through the hub to the blades - allowed no leakage. The present arrangement, however, with graphite seals placed between fixed and rotating parts may allow considerable leakage, especially at the velocities encountered in the tunnel throat at the higher blade angles.

The consideration of the pressure field about the spinner and the probability that the internal pressure at the graphite seals is elevated by centrifugal effects lead to the belief that the leakage is outward. When leakage takes place from the spinner to the surrounding atmosphere, the actual mass flow is less than the measured internal mass flow, and the measured mass-flow coefficients are therefore too high. Referring to equation (26) of reference 2, which is

$$\frac{\Delta p_f}{q_N} = \left(\frac{\rho_N}{\rho}\right)^2 \frac{\left[(\pi x)^2 + J^2\right]}{m_c^2} - 1$$

and noting that ρ_N/ρ is practically constant (table I) indicates that $\Delta p_f/q_N$ would be greatly influenced by errors in the measurement of m_c.

Another factor influencing the value of m_c, and therefore of $\Delta p_f/q_N$ and ρ_N/ρ, is the selection of a value of A_N' to be used in the computations. The value of A_N' used was that determined from the smoke tests. These tests, however, were performed under static conditions, and the actual value of A_N' may vary, depending on rotational speed (centrifugal pumping action) and the variation in the aerodynamic suction at the tip nozzle.

Design mass-flow coefficient.- The correct values of design mass flow could not be used in these tests because of the limited throttle closure previously mentioned. The correct weight flow has been established for a typical flight application for these particular blades to be 0.10 pound per second at 700 feet per second rotational tip speed when 350° F air is delivered to the blade shanks at 15,000 feet altitude. The dashed lines in figures 15(a) and 15(b) are the values of design m_c based on the aforementioned figures and on the same nozzle area as was assumed in the computation of actual m_c. The assumption has also been made that the air flow will vary in direct proportion to the altitude density and propeller rotational speed. When these assumptions are adopted, m_c becomes a constant. Actually m_c increases with increasing J. One reason for this increase is that ram has been neglected in the computation of design m_c. Another factor tending to increase m_c with increasing J is the effective nozzle area. The nozzle area has been assumed constant, but there may be a reduction in effective nozzle area at the higher velocities.

For a given rotational speed (1350 rpm), m_c, as defined, varied from approximately 20 percent to 120 percent greater than the design m_c. This variation depended on the value of J.

Calculated efficiency losses.- The values of $\Delta p_f/q_N$, ρ_N/ρ, and m_c lead to the computation of efficiency losses caused by the tip-nozzle drag and internal flow. An expression for the over-all change in efficiency has been presented in equation (21) of reference 2 as follows:

$$\Delta\eta = \frac{A_N'}{D^2}\frac{\eta}{C_P}\left[(\pi x)^2 + \frac{J^2}{\eta}\right]\left\{m_c\left[\frac{\rho}{\rho_N}\frac{m_c\epsilon}{\sqrt{(\pi x)^2 + J^2}} - 1\right] - \frac{C_{D_N}}{2}\sqrt{(\pi x)^2 + J^2}\right\}$$

Appropriate values for the quantities A_N', ϵ, and C_{D_N} have been assumed. The values of A_N' and ϵ were estimated from the smoke-flow

tests. The maximum value of C_{D_N} was taken as 0.57 (fig. 16). This value was determined in previous tests (unpublished) of a similar nozzle.

The values of $\Delta\eta$ at the maximum efficiency calculated from the combined-loss equation and those values obtained from the curves of force data are both presented in table I. The results may be considered in fair agreement. It should be kept in mind that individual force data may be repeated only to the nearest 1 percent.

Torque of Graphite Seals

The graphite seals used to reduce leakage at the spinner juncture are inevitably a source of power loss. To determine exactly the magnitude of the power losses for this particular installation was desired. These seals operated on a diameter of 23.562 inches. The torque was determined by readings of the torquemeter with the seals in and again with the seals out at which time the propeller was allowed to wind-mill in the tunnel stream. The torque required to overcome the seal friction was found to be 19.4 foot-pounds at all rotational speeds, or 5 horsepower at 1350 rpm. This rotational drag would depend on the pressure difference across the seal, the diameter of the seal, and the amount of effective lubrication.

For the peak-efficiency condition at a blade angle of 40°, the rotational drag when charged to the propeller resulted in an additional $6\frac{1}{2}$ percent decrease in efficiency, or a net efficiency of 0.844. By comparison, the losses entailed by the introduction of tip nozzle and internal air flow may be considered of small importance.

CONCLUSIONS

The following conclusions were indicated by tests to determine the effects on propeller efficiency of thermal de-icing of airplane propellers by use of internal flow through hollow blades:

1. Flow through a tip nozzle of good external design but with poor internal ducting caused peak efficiency losses of little more than 1 percent.

2. The peak efficiency losses may be estimated with fair accuracy by the use of a theoretical method.

3. The addition of heat to the internal flow caused no appreciable additional change in the envelope efficiency.

4. Bench tests indicated that changes in blade angle did not effect the pressure drop through the system.

5. Bench tests employing smoke indicated that the internal ducting of the blade should be faired to the tip nozzle to obtain better flow characteristics.

6. The torque of the spinner-juncture seals necessary to this design was excessive and large efficiency losses resulted when this torque was charged to the propeller.

Langley Memorial Aeronautical Laboratory
National Advisory Committee for Aeronautics
Langley Field, Va., September 27, 1947

REFERENCES

1. Corson, Blake W., Jr., and Maynard, Julian D.: Investigation of the Effect of a Tip Modification and Thermal De-Icing Air Flow on Propeller Performance. NACA TN No. 1111, 1946.

2. Corson, Blake W., Jr., and Maynard, Julian D.: Analysis of Propeller Efficiency Losses Associated with Heated-Air Thermal De-Icing. NACA TN No. 1112, 1946.

3. Corson, Blake W., Jr., and Maynard, Julian D.: The Effect of Simulated Icing on Propeller Performance. NACA TN No. 1084, 1946.

4. Brigham, W. E.: Heated Air Thermal Anti-Icing Flight Tests of Curtiss Electric Propellers with Hollow Steel Blades. Rep. No. C-1635, Curtiss-Wright Corp., Propeller Div. (Caldwell, N. J.), Sept. 13, 1945, p. 78.

TABLE I

EFFICIENCY LOSS AT PEAK EFFICIENCY

$\left[A_N' = 0.00544 \frac{1}{\cos 31^\circ} = 0.00635 \text{ sq ft};\ D = 10.19 \text{ ft};\ x = 0.996;\ C_{D_N} = 0.57;\ \epsilon = 0.86;\ N = 1350 \text{ rpm}\right]$

β at 42-inch radius	J	η for uncut blades	C_P for uncut blades	m_c		$\Delta p_f/q_N$		ρ/ρ_N		$\Delta\eta$			
										Measured		Calculated	
				Cold	Heated	Cold	Heated	Cold	Heated	Cold	Heated	Cold	Heated
20	0.770	0.876	0.0335	1.841	-----	1.763	-----	1.053	-----	0.007	------	-0.032	------
25	.950	.906	.0514	1.990	1.825	1.449	1.882	1.051	1.055	-----	-0.003	- .023	-0.023
30	1.230	.920	.0653	2.195	2.020	1.137	1.492	1.048	1.054	-0.013	- .010	- .020	- .020
35	1.430	.920	.0928	2.413	2.225	.865	1.164	1.044	1.051	- .008	- .008	- .015	- .015
40	1.640	.919	.1289	2.605	2.440	.691	.910	1.043	1.048	- .011	- .012	- .012	- .012
45	2.015	.910	.1689	2.976	2.720	.464	.713	1.034	1.045	- .010	- .010	- .010	- .011
[a]50	2.310	.900	.2279	3.254	2.980	.381	.627	1.017	1.023	- .012	- .013	- .009	- .009
[a]55	2.750	.896	.3386	3.595	3.184	.301	.625	1.016	1.026	- .016	- .011	- .007	- .008
Bench test	-----	-----	------	-----	-----	0.335	-----	1.156	-----	------	------	------	------

[a] N = 1140 rpm for uncut blades and 960 rpm for tests with flow.

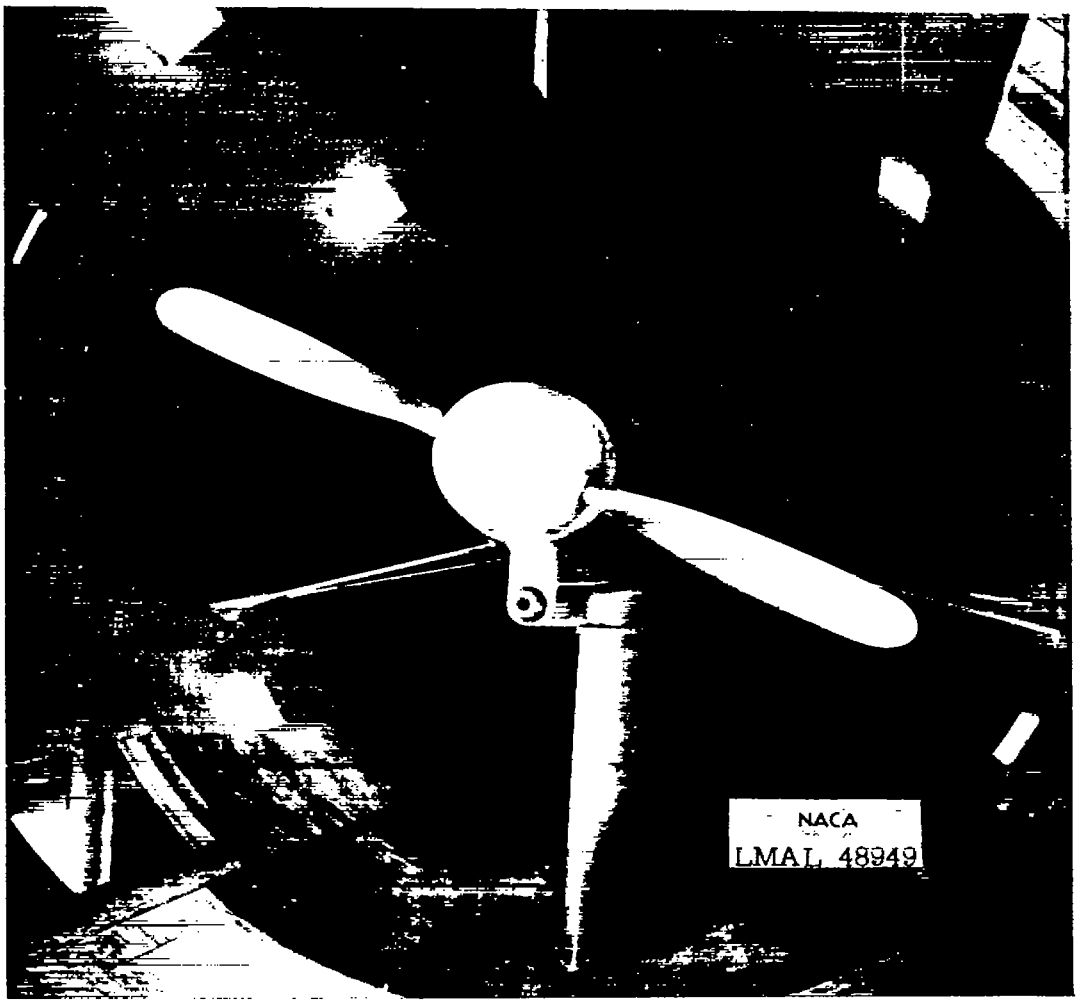

Figure 1.- Wind-tunnel test arrangement.

NATIONAL ADVISORY COMMITTEE FOR AERONAUTICS
LANGLEY MEMORIAL AERONAUTICAL LABORATORY - LANGLEY FIELD, VA.

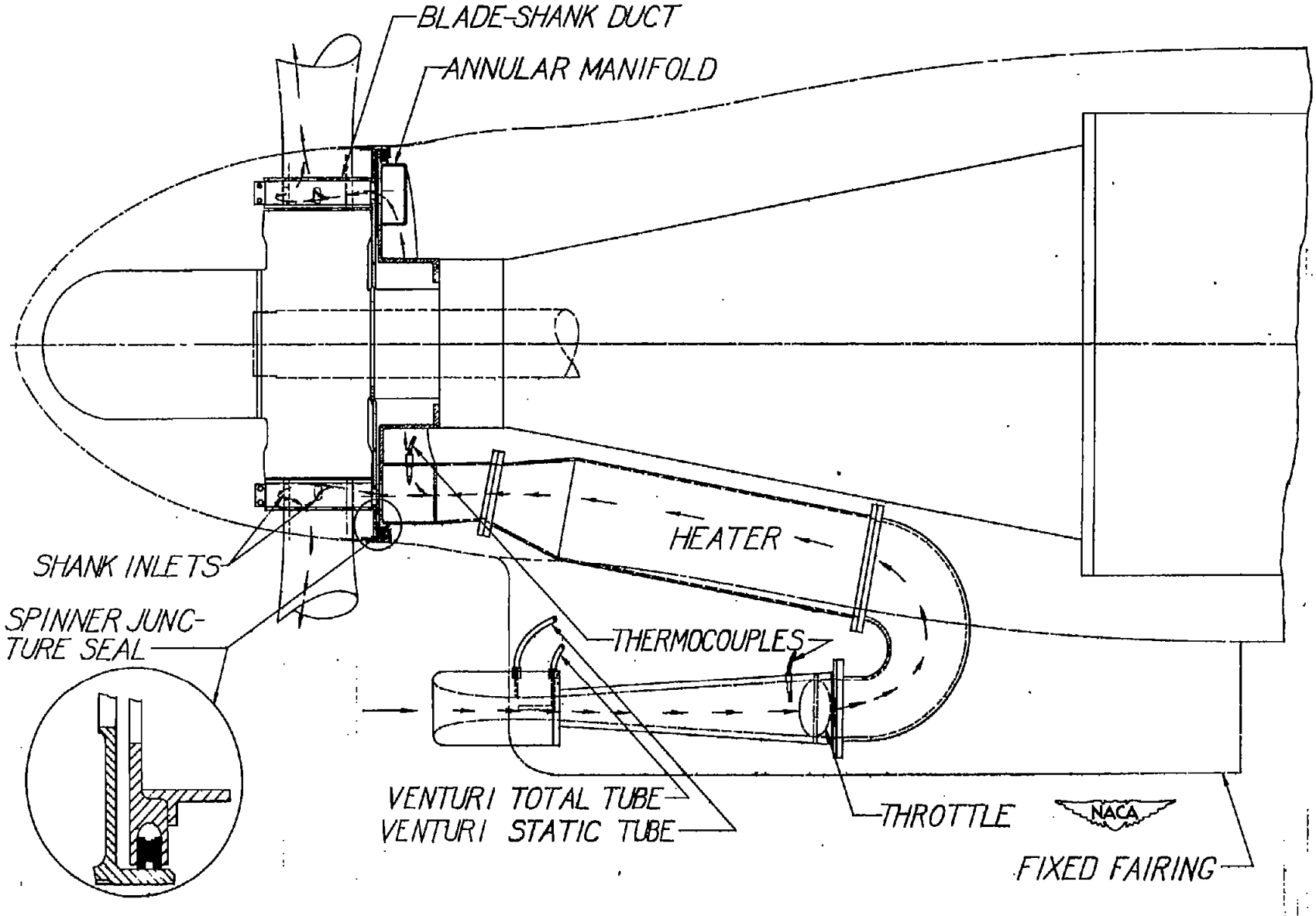

FIGURE 2.—INTERNAL AIRFLOW SYSTEM OF WIND-TUNNEL TEST SETUP.

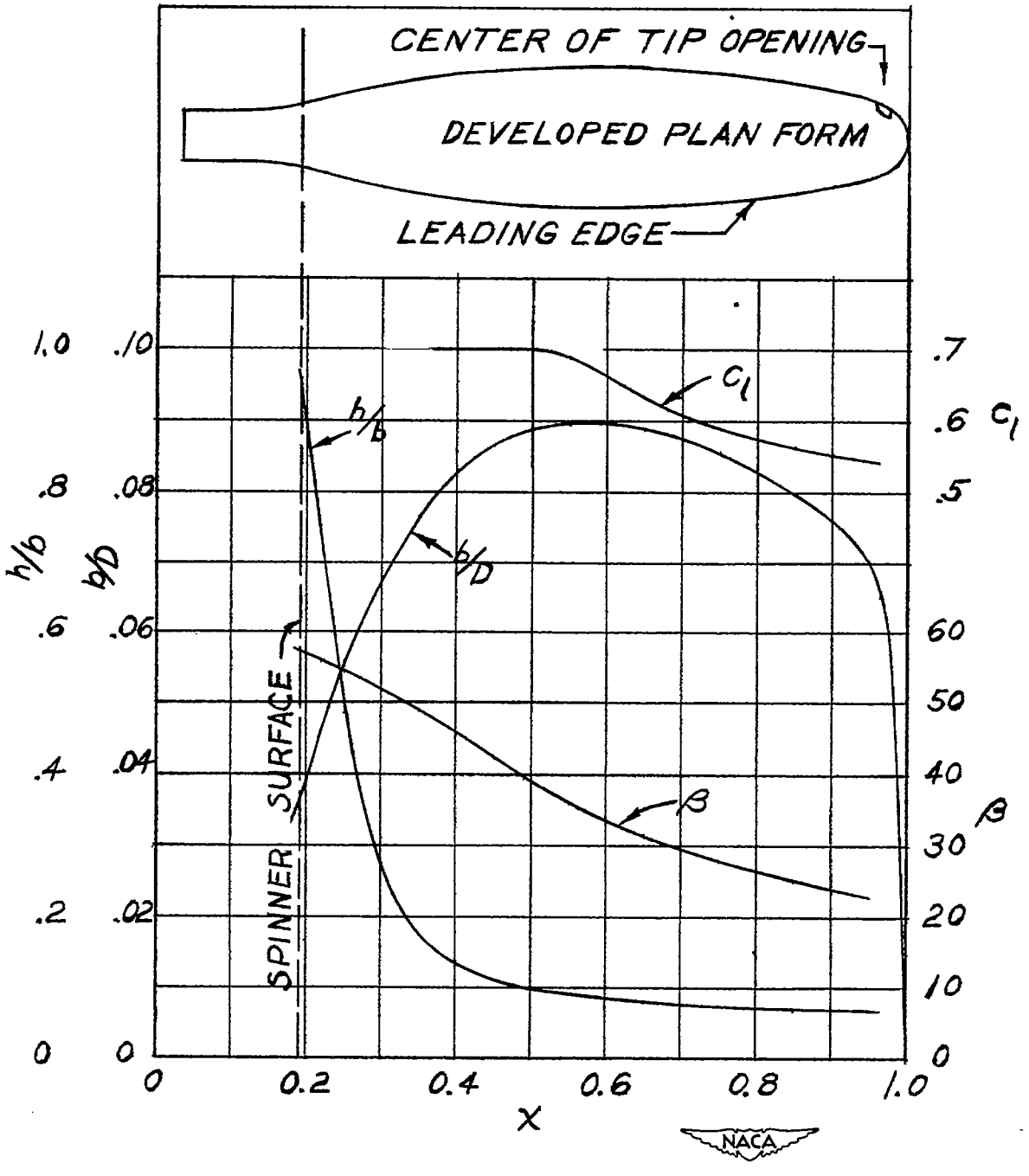

Figure 3.—Blade-form curves for the propeller tested.

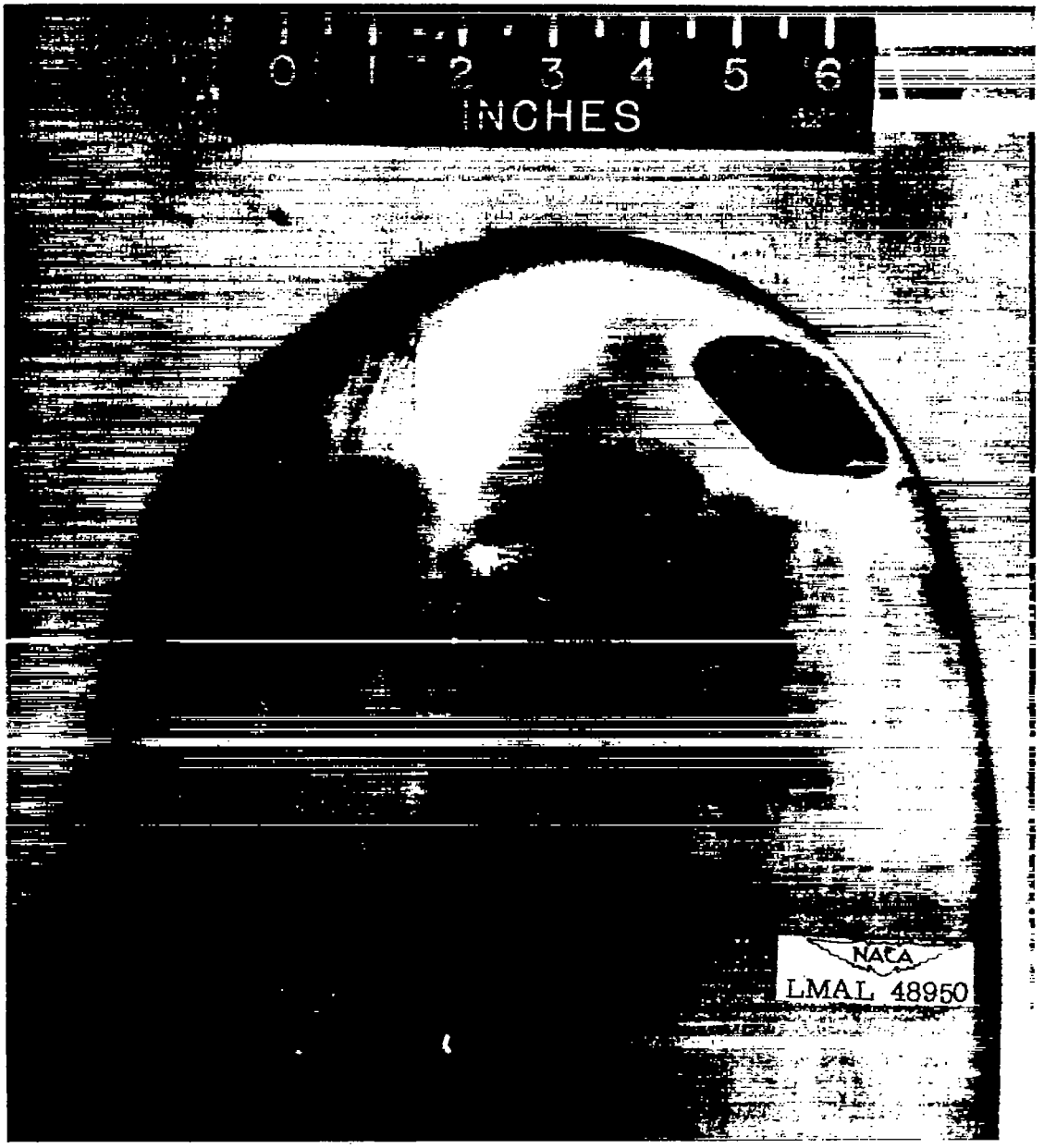

Figure 4.- Blade tip and tip nozzle.

NATIONAL ADVISORY COMMITTEE FOR AERONAUTICS
LANGLEY MEMORIAL AERONAUTICAL LABORATORY - LANGLEY FIELD, VA

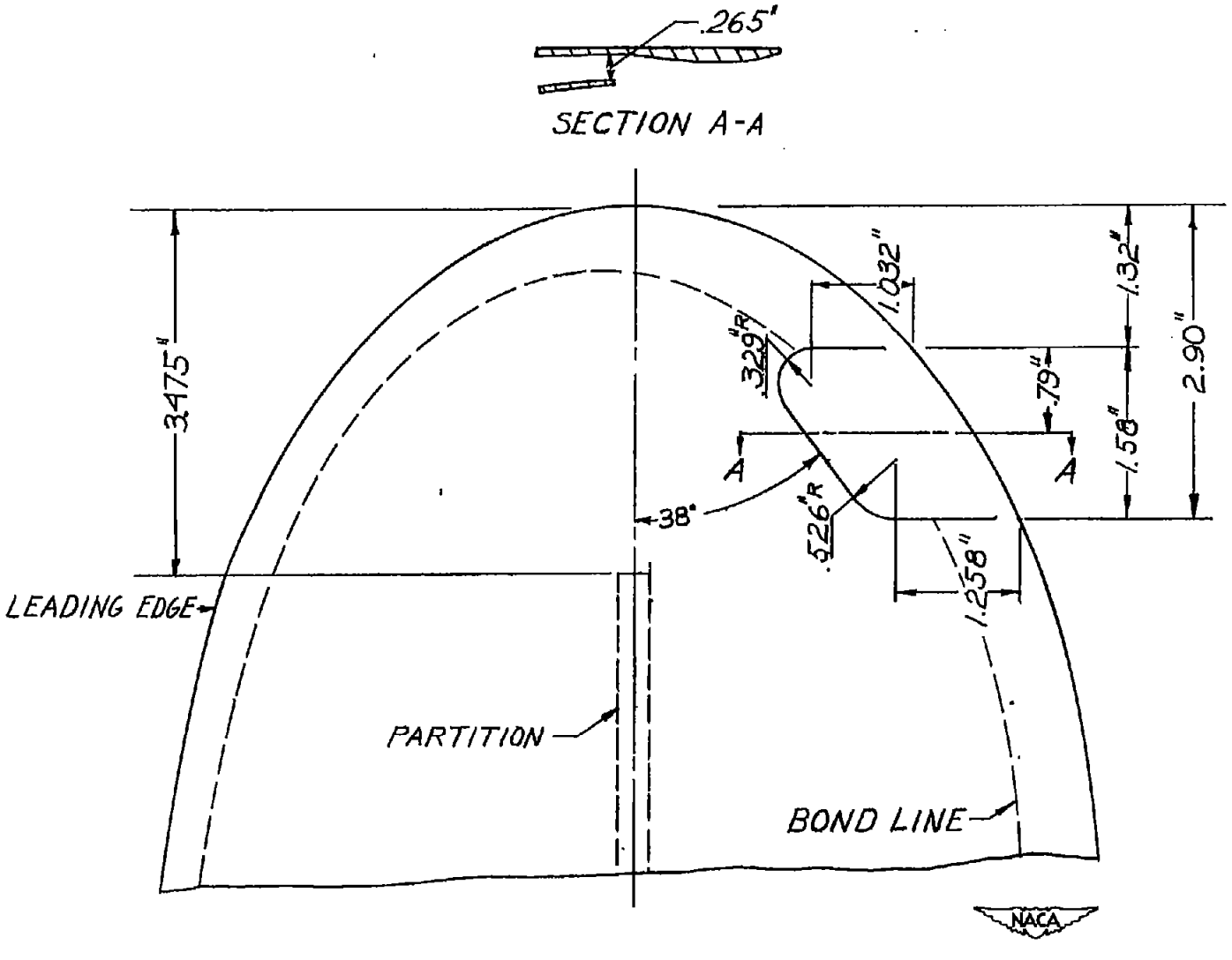

FIGURE 5.—THERMAL DE-ICING PROPELLER TIP NOZZLE.

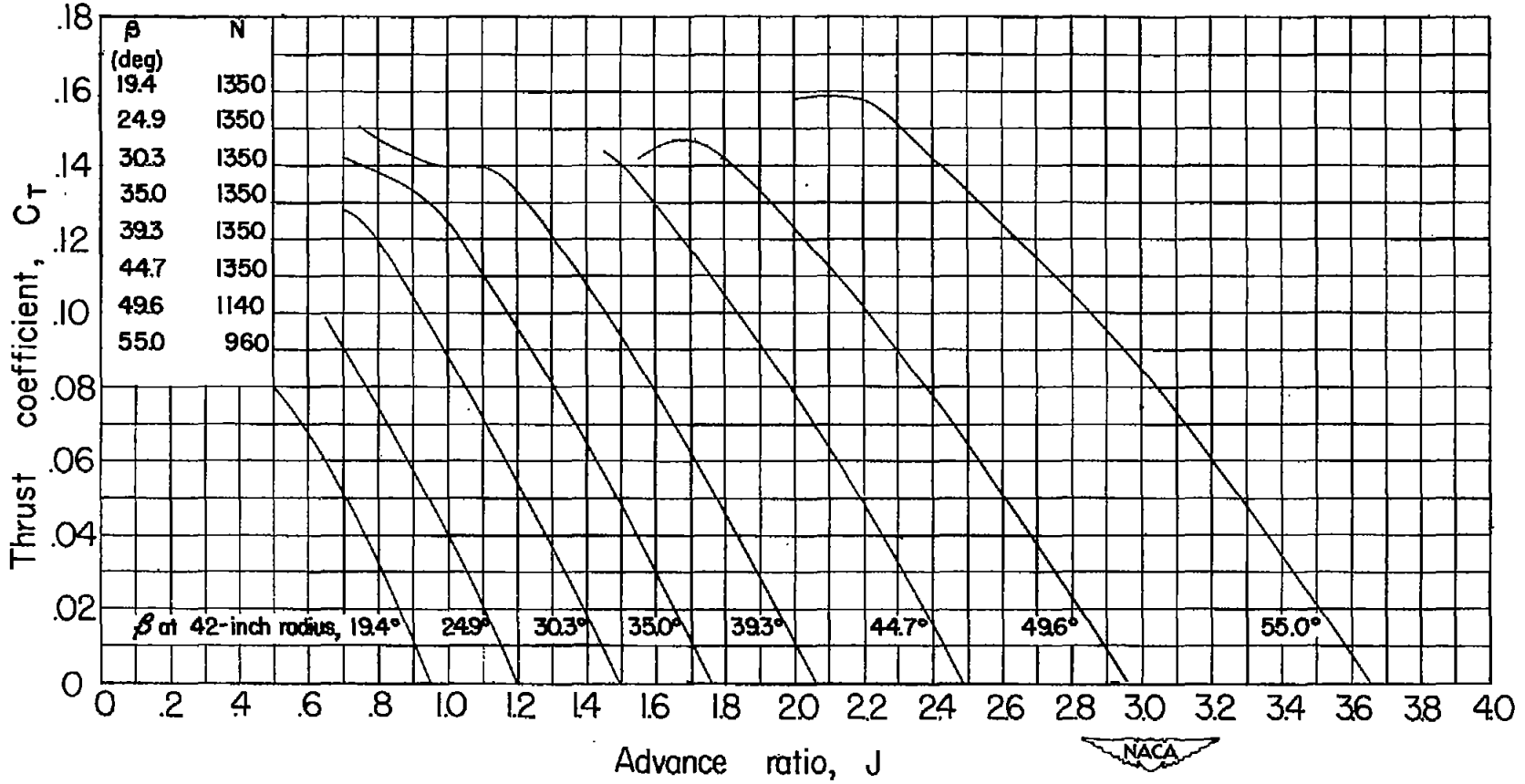

(a) Thrust coefficient.

Figure 6 .— Propeller aerodynamic characteristics with no internal flow.

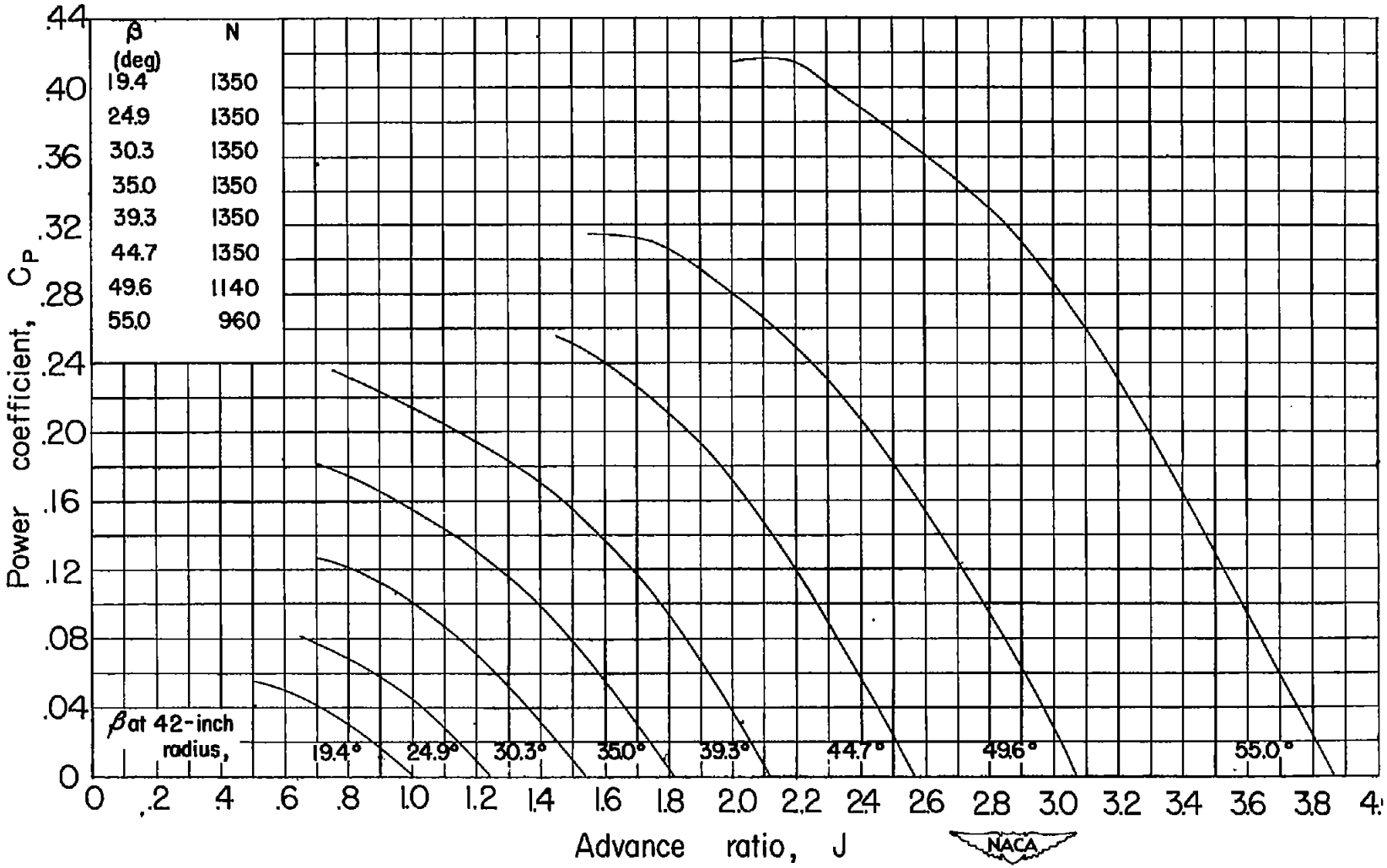

(b) Power coefficient.

Figure 6 .—Continued.

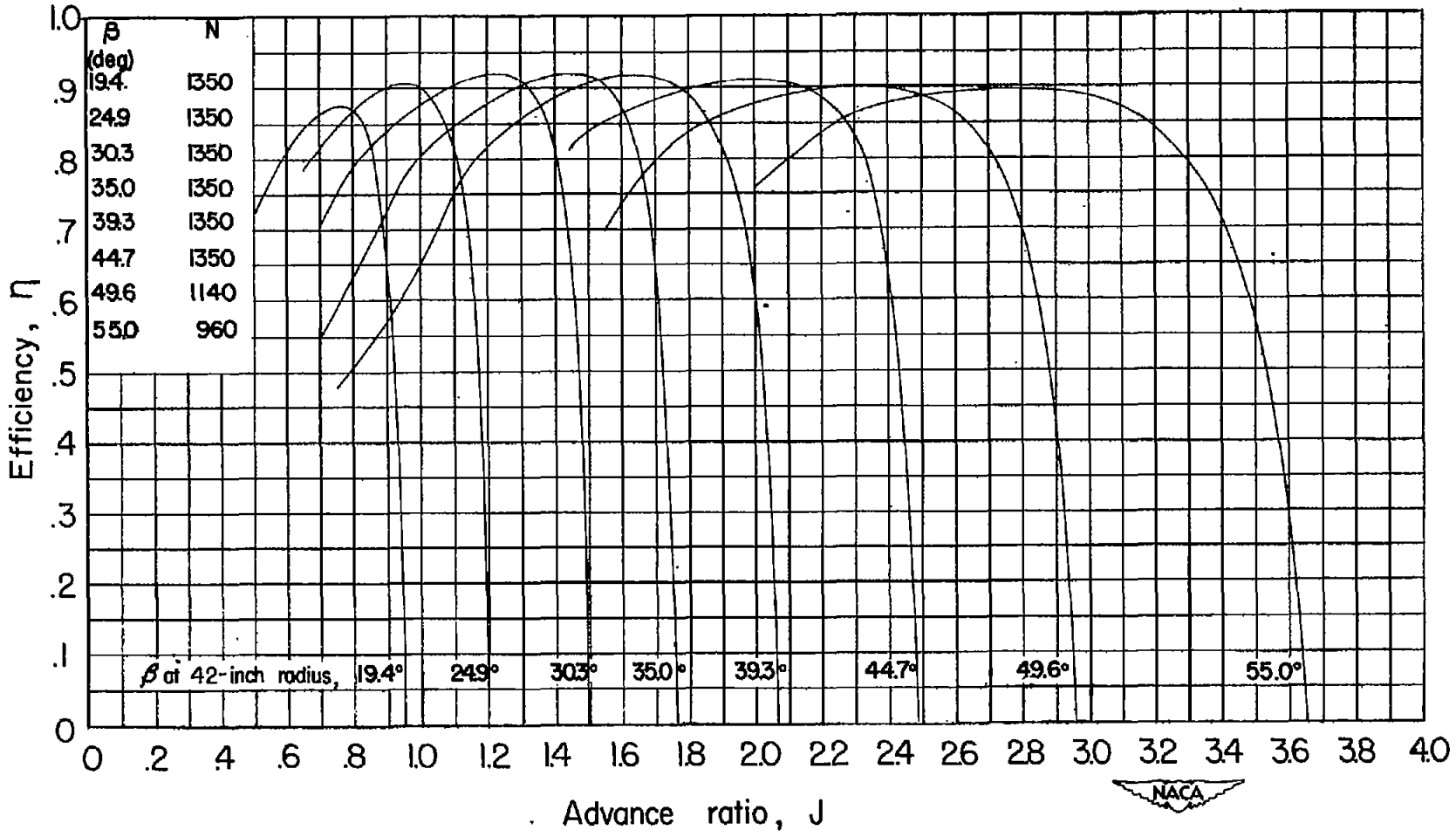

(c) Efficiency.

Figure 6 .— Concluded.

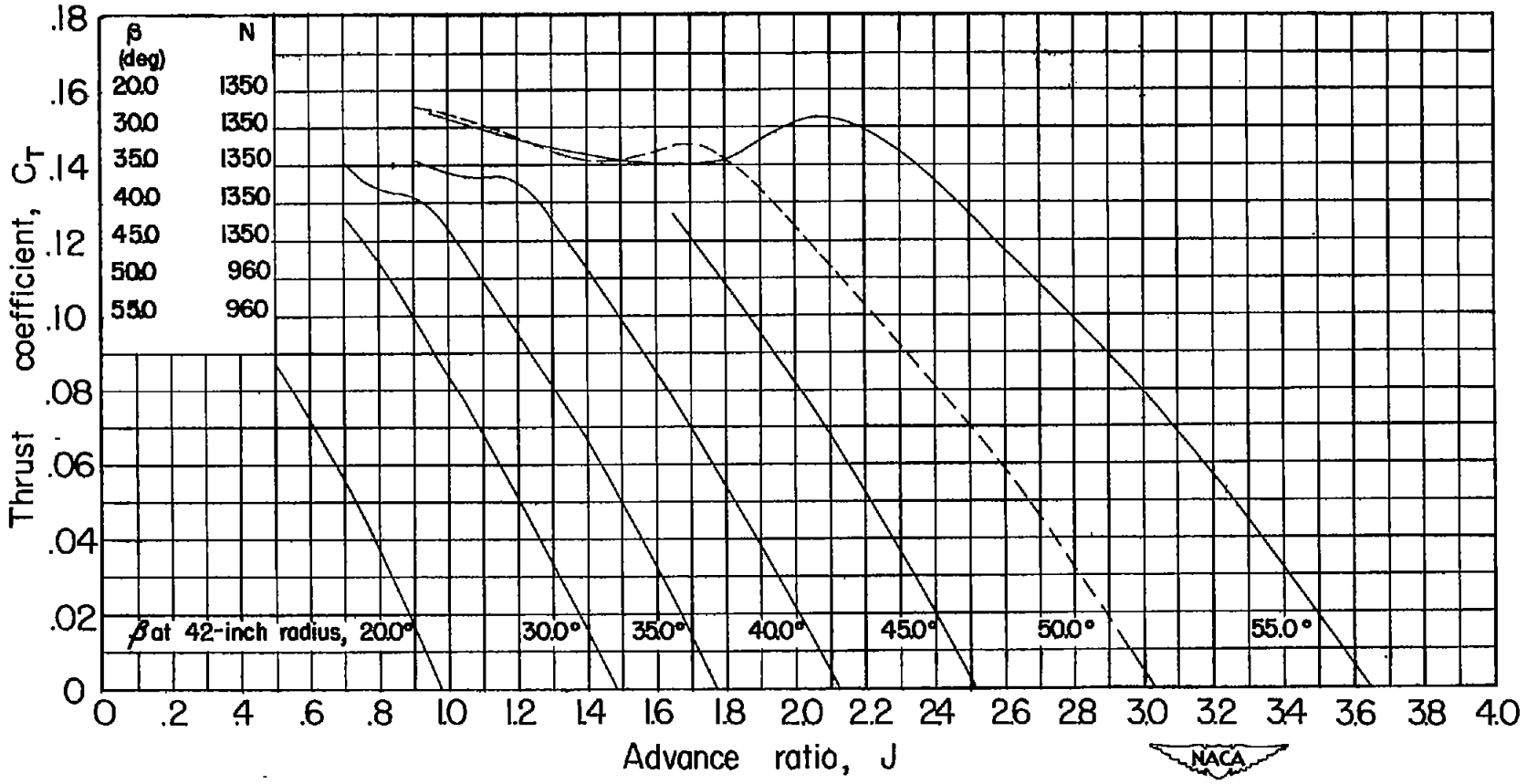

(a) Thrust coefficient.

Figure 7.— Propeller aerodynamic characteristics with cold internal flow.

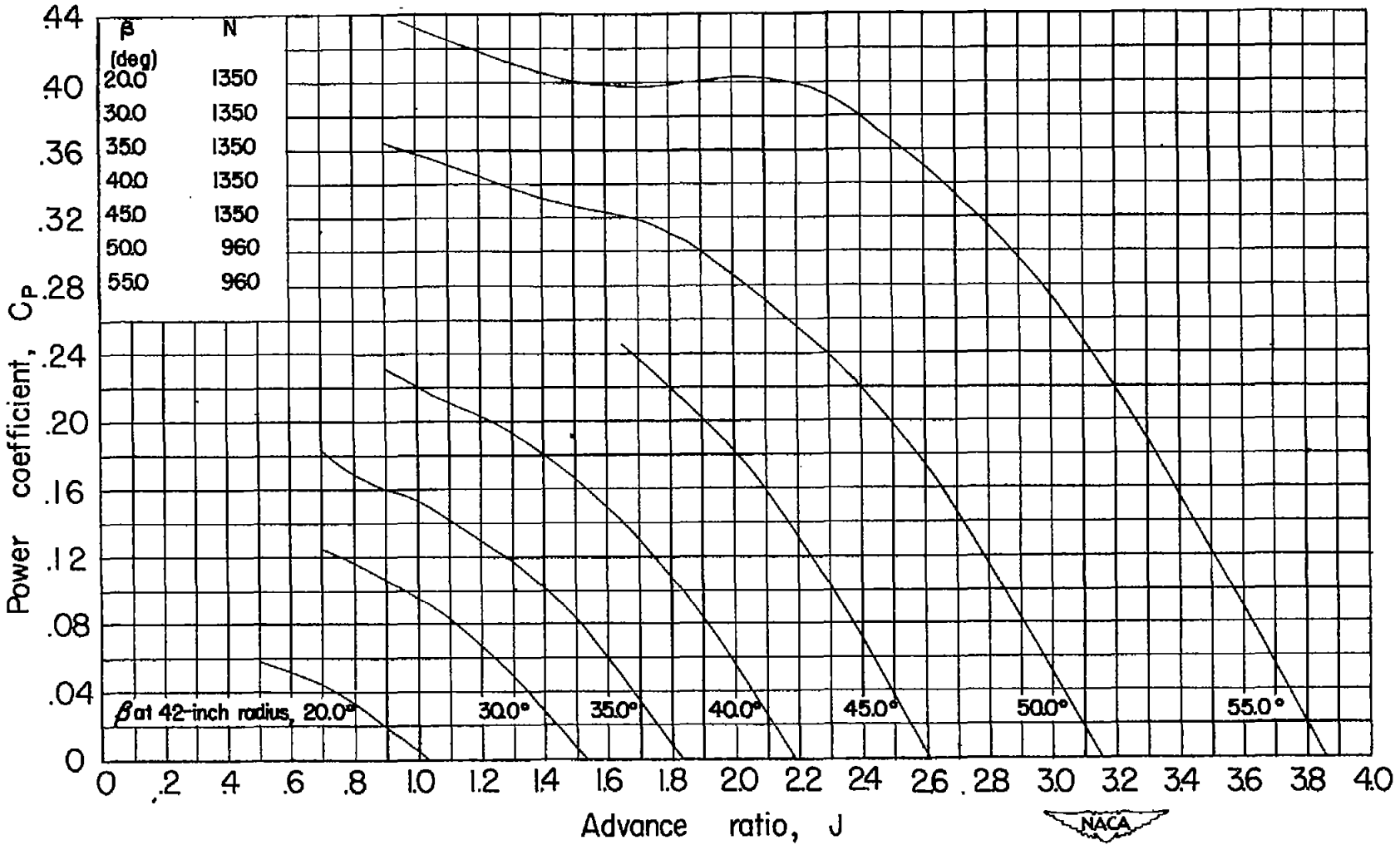

(b) Power coefficient.

Figure 7.— Continued.

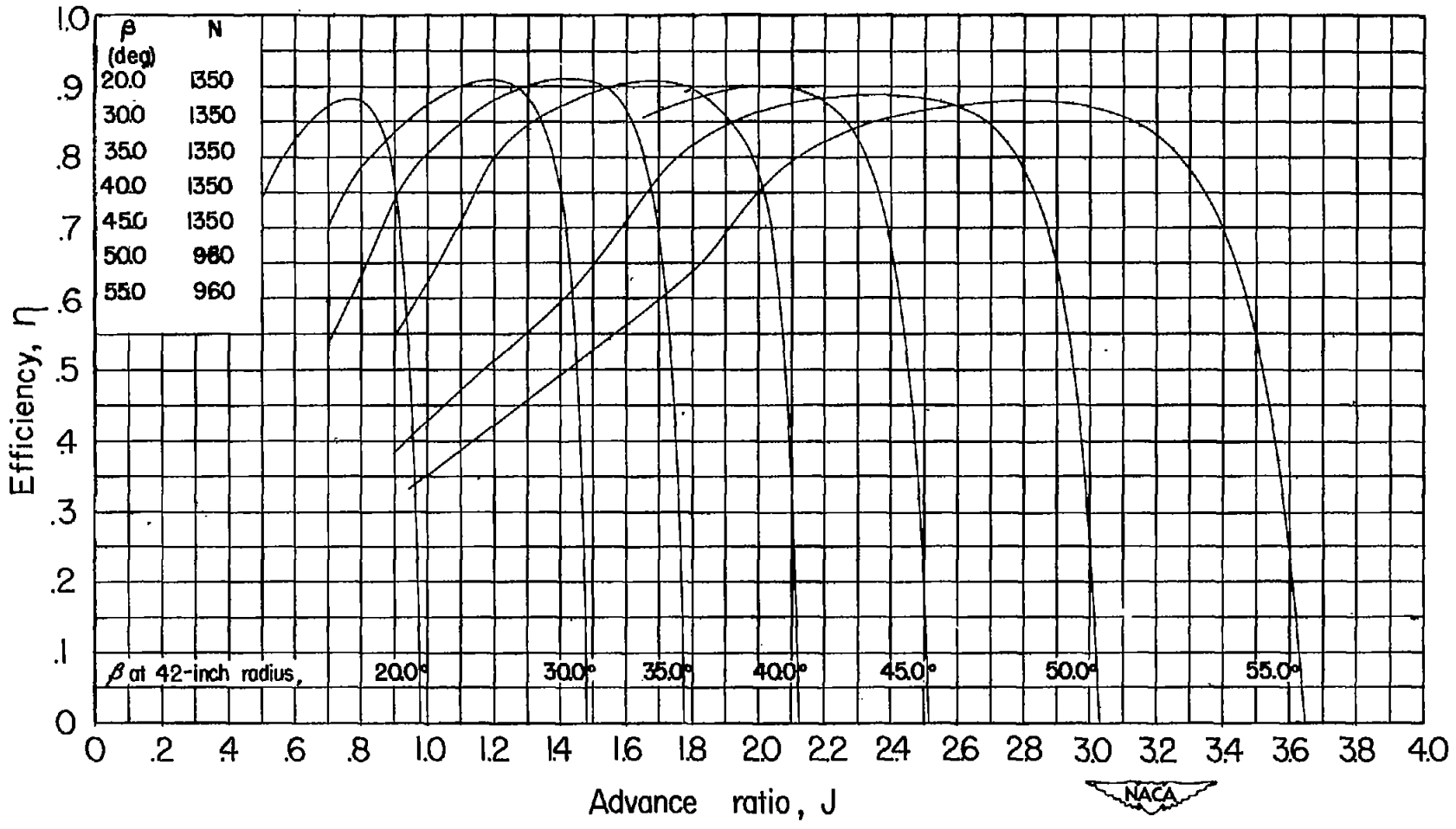

(c) Efficiency.

Figure 7 .— Concluded.

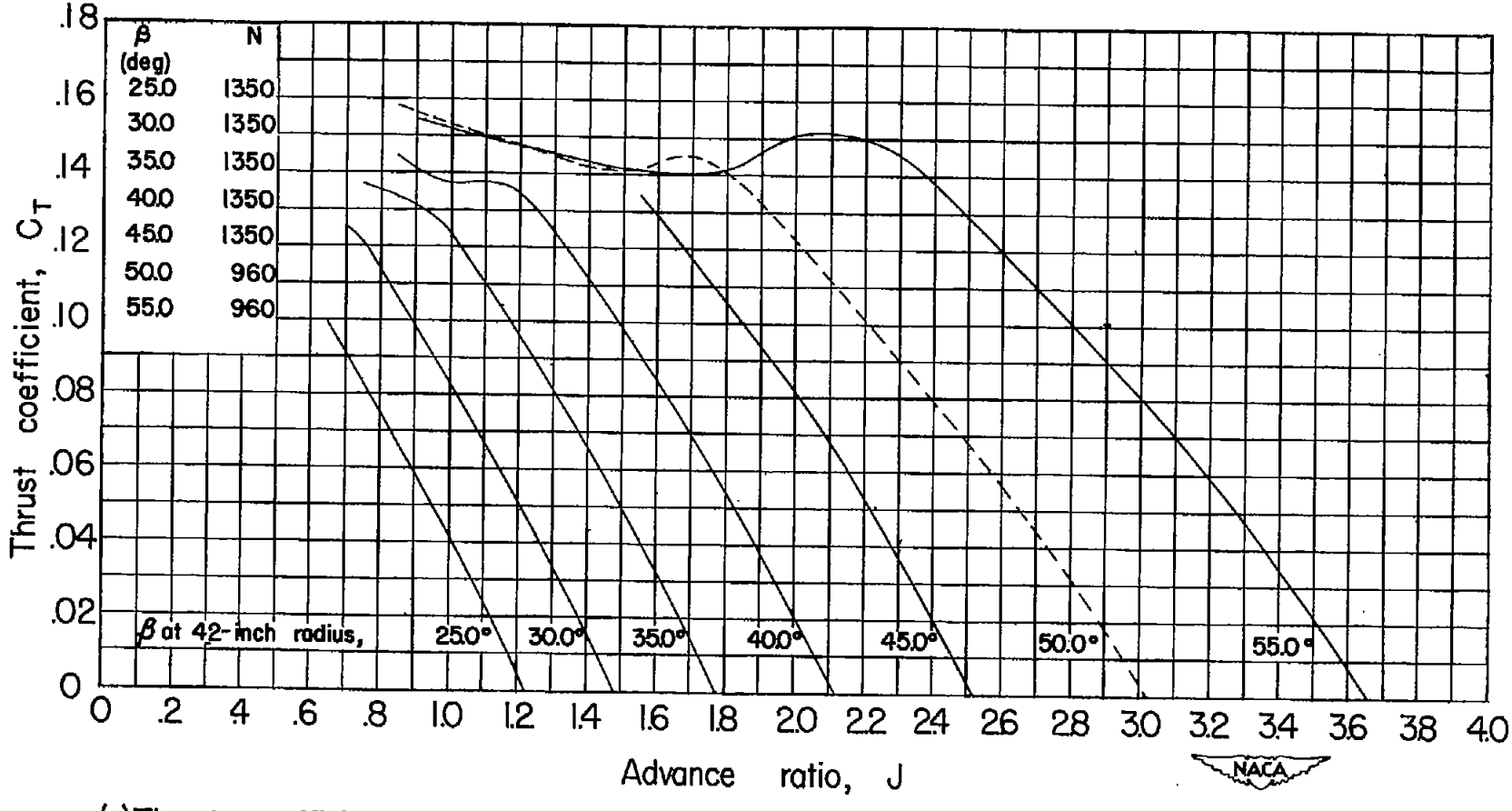

(a) Thrust coefficient.

Figure 8 .—Propeller aerodynamic characteristics with heated internal flow.

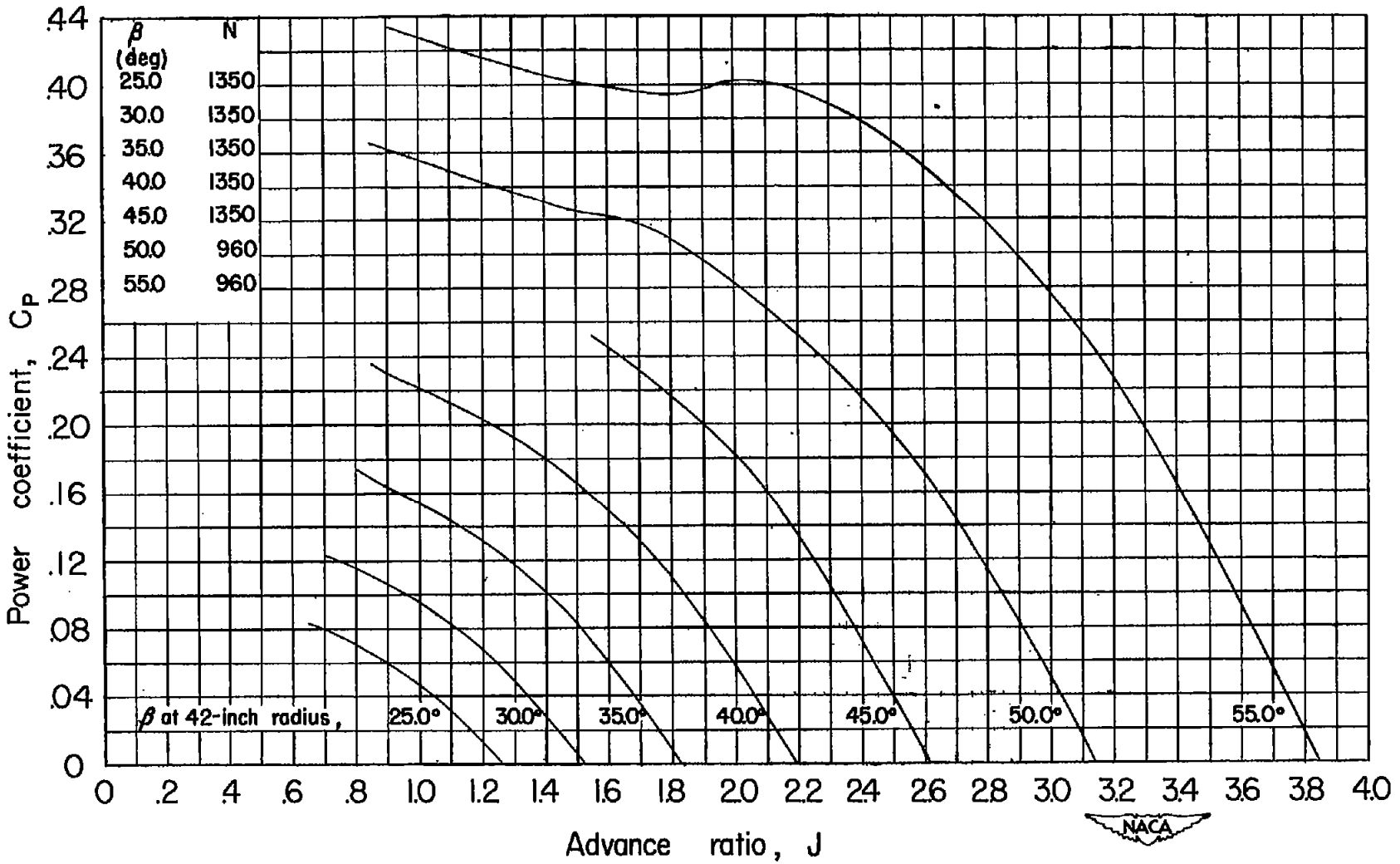

(b) Power coefficient.

Figure 8 .— Continued.

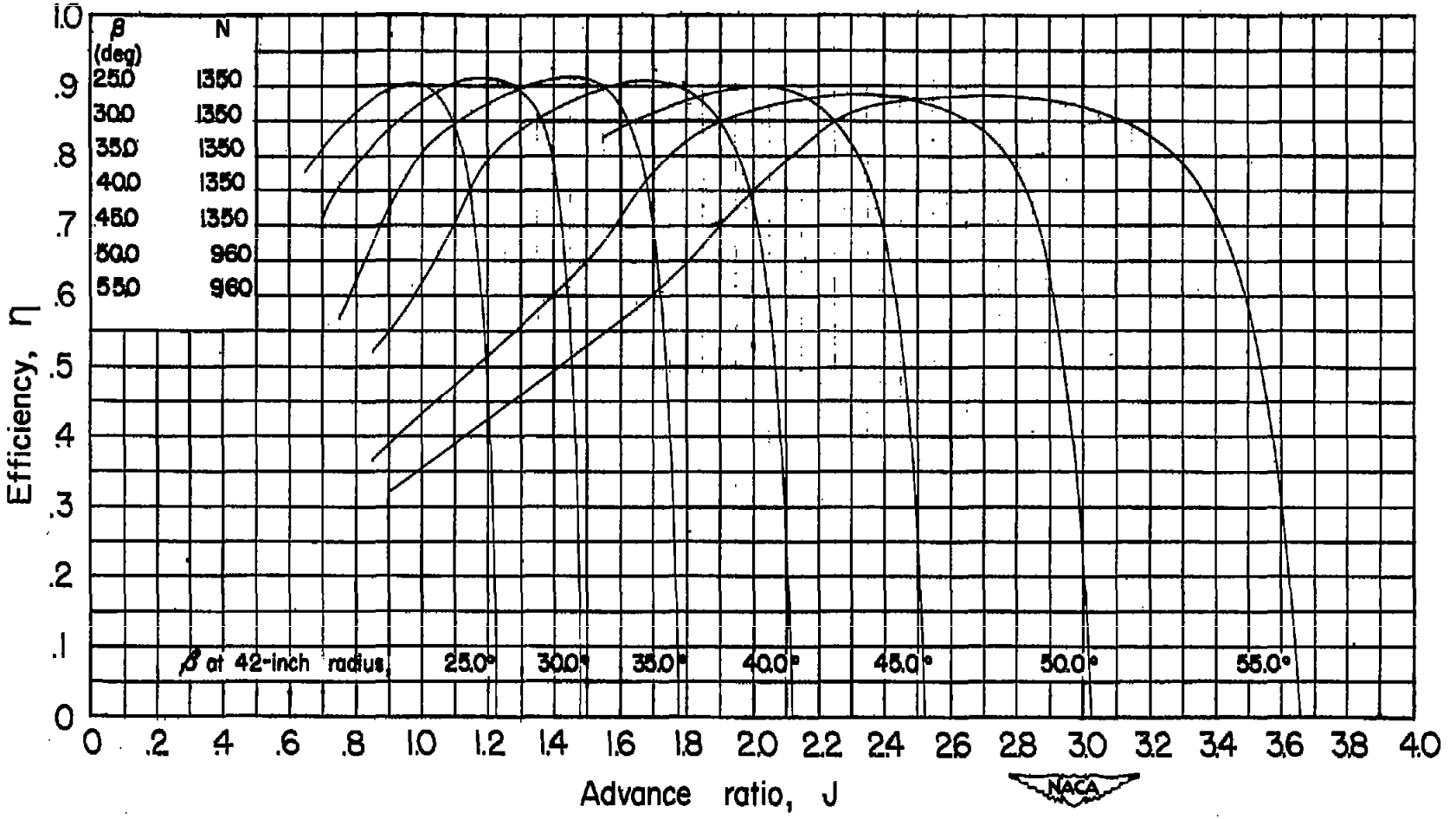

(c) Efficiency.

Figure 8 .— Concluded.

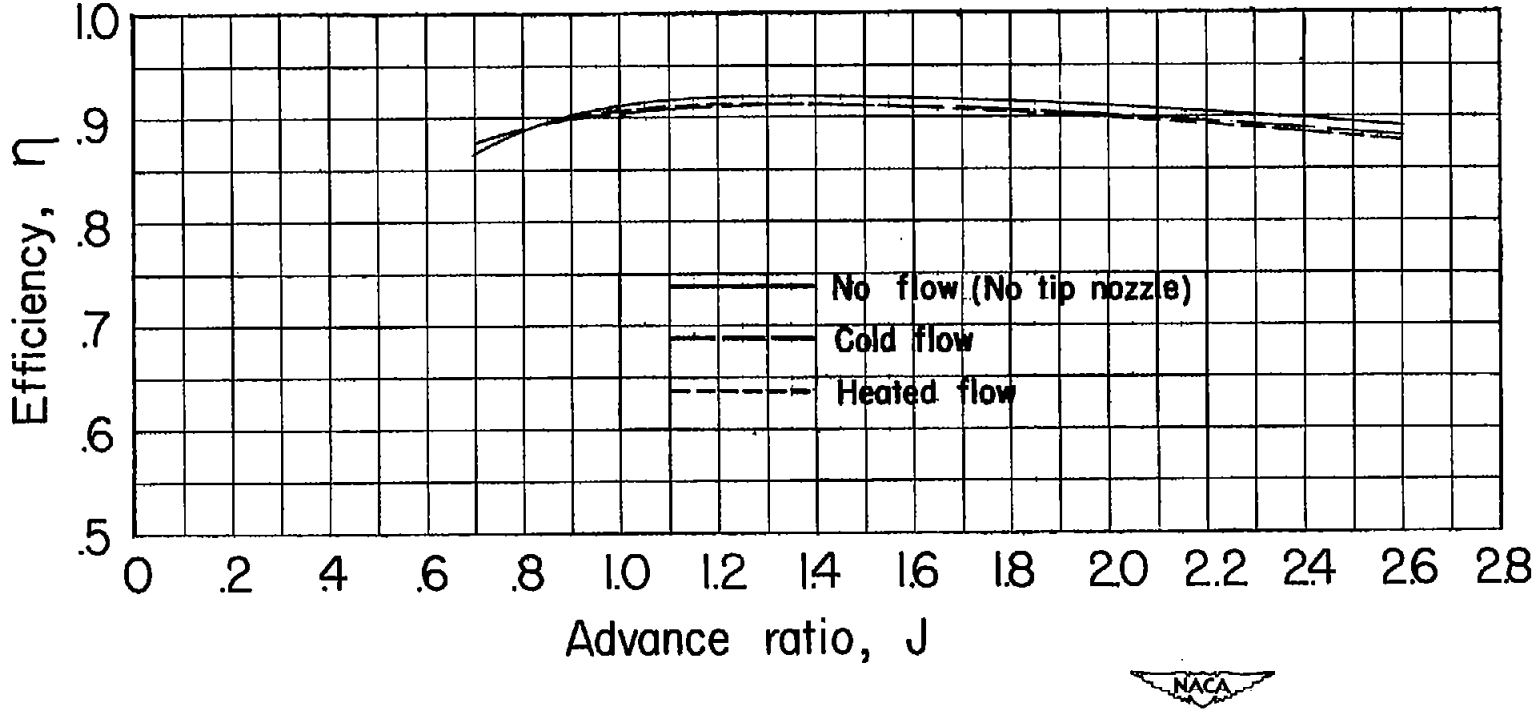

Figure 9.—Effect of internal flow on envelope efficiency.

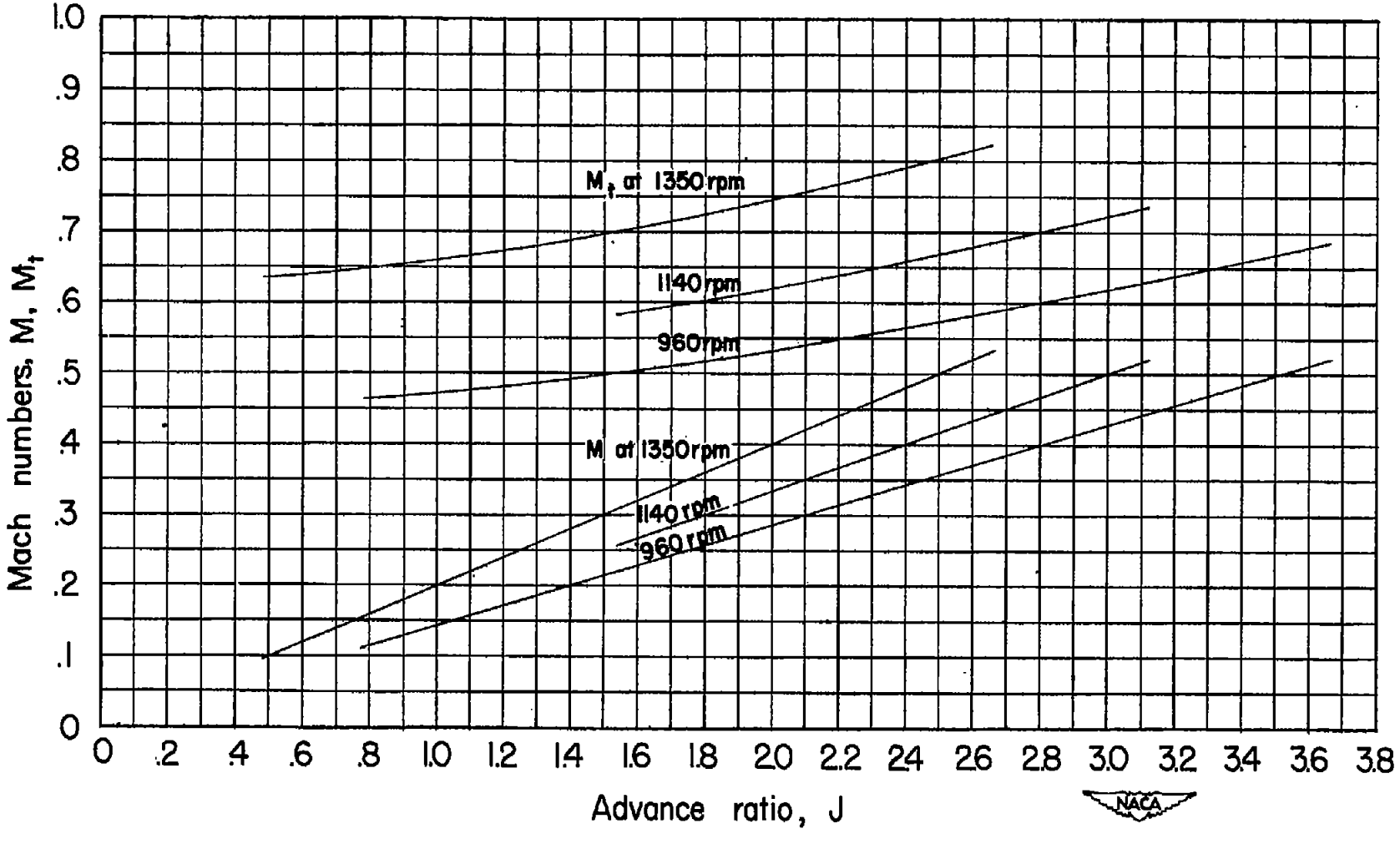

Figure 10.—Variation of air-stream Mach number and helical tip Mach number with advance ratio.

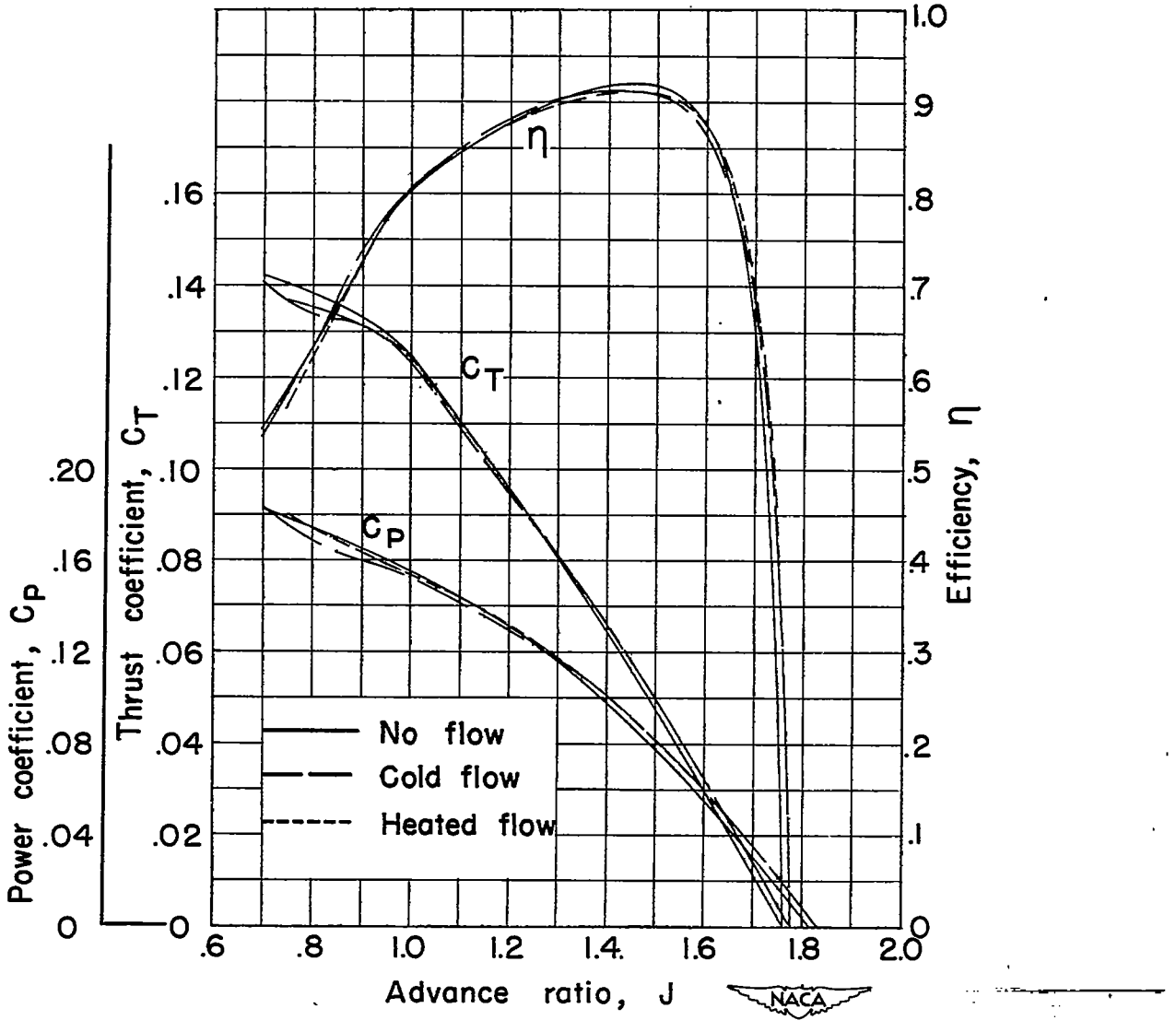

Figure 11.— Effect of internal flow on propeller characteristics, $\beta = 35.0°$.

(a) Top view.

Figure 12.- Flow from blade tip nozzle.

NATIONAL ADVISORY COMMITTEE FOR AERONAUTICS
LANGLEY MEMORIAL AERONAUTICAL LABORATORY - LANGLEY FIELD, VA

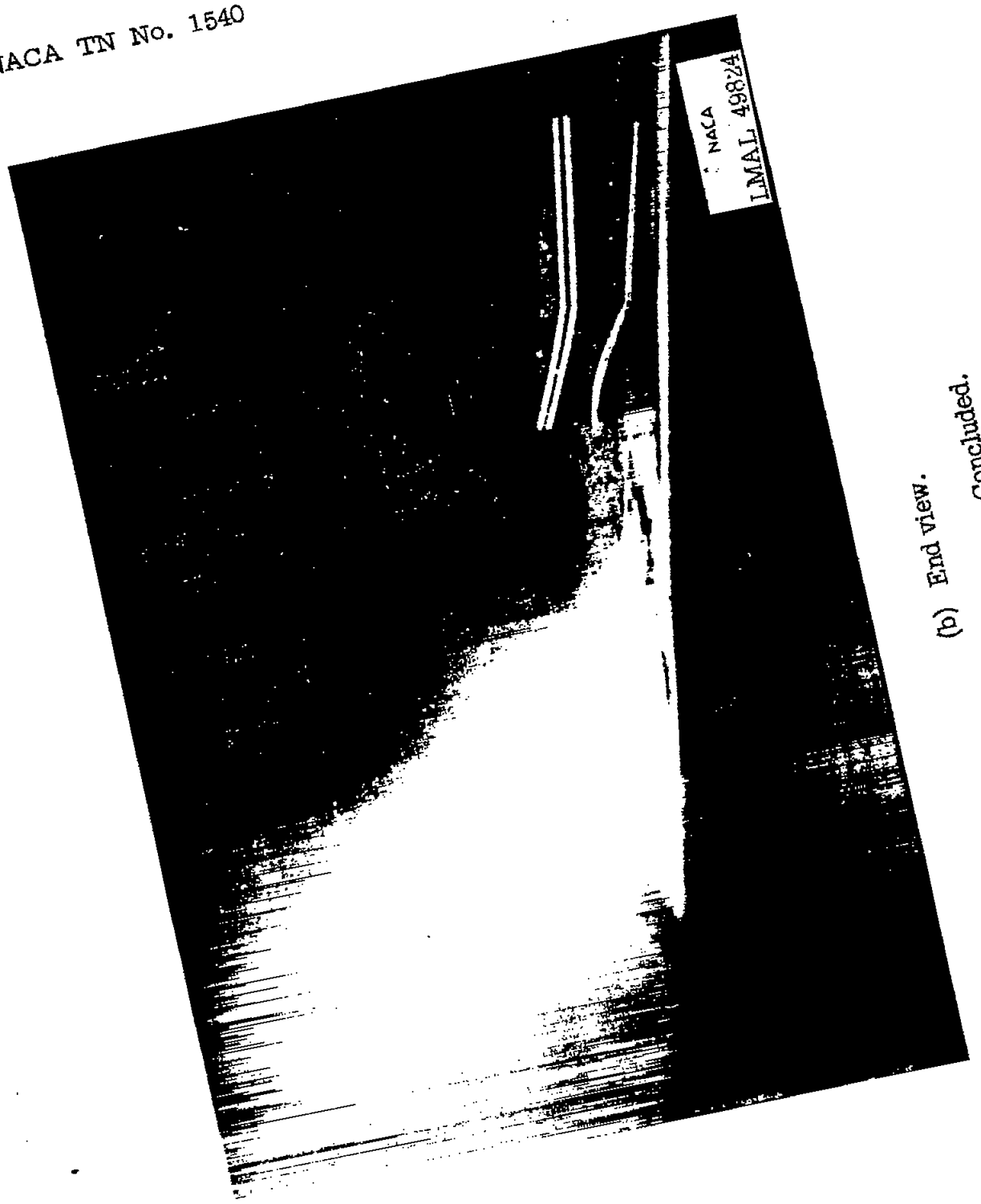

(b) End view.

Figure 12.- Concluded.

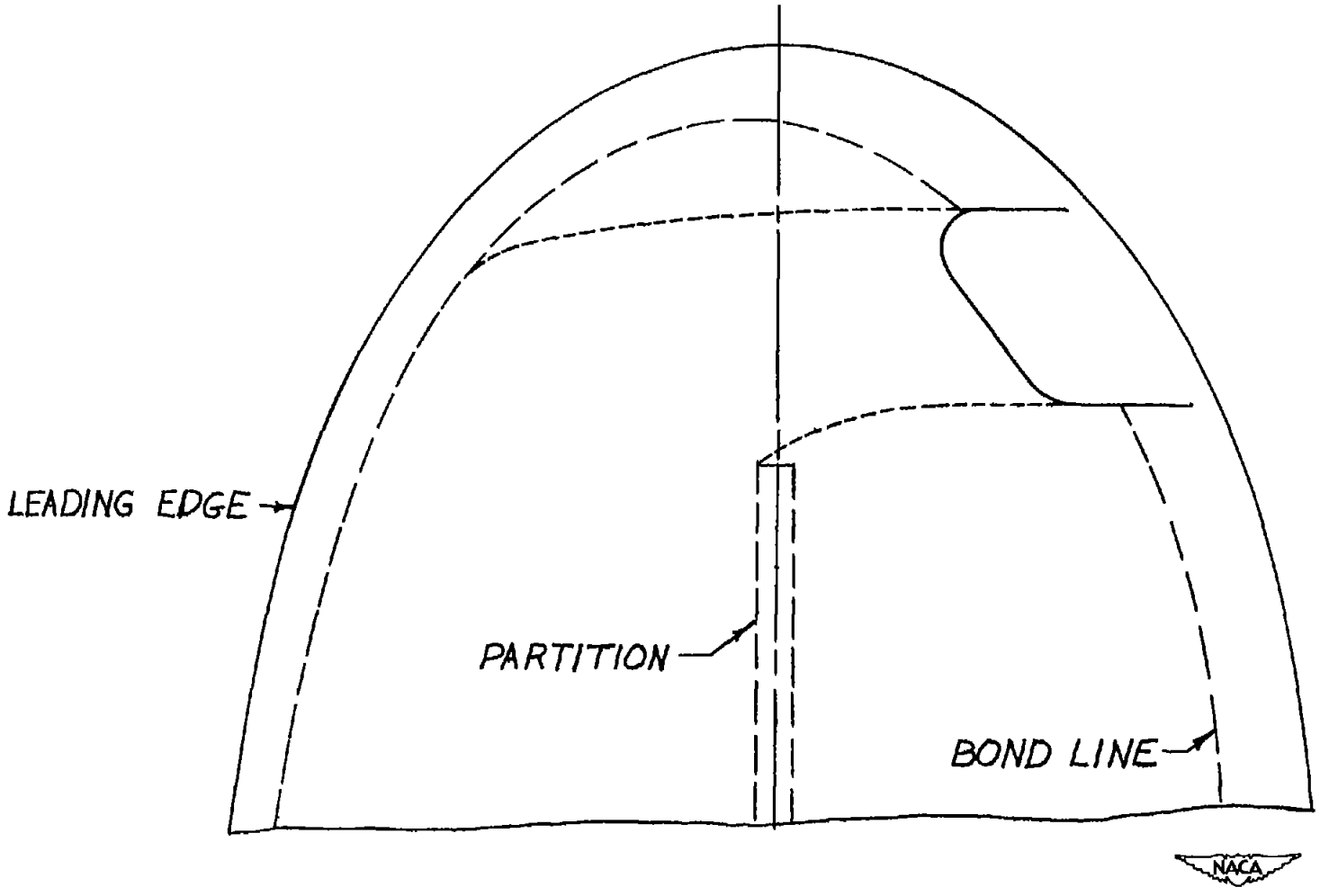

FIGURE 13.—FAIRING LINES FOR REVISED BLADE-TIP NOZZLE.

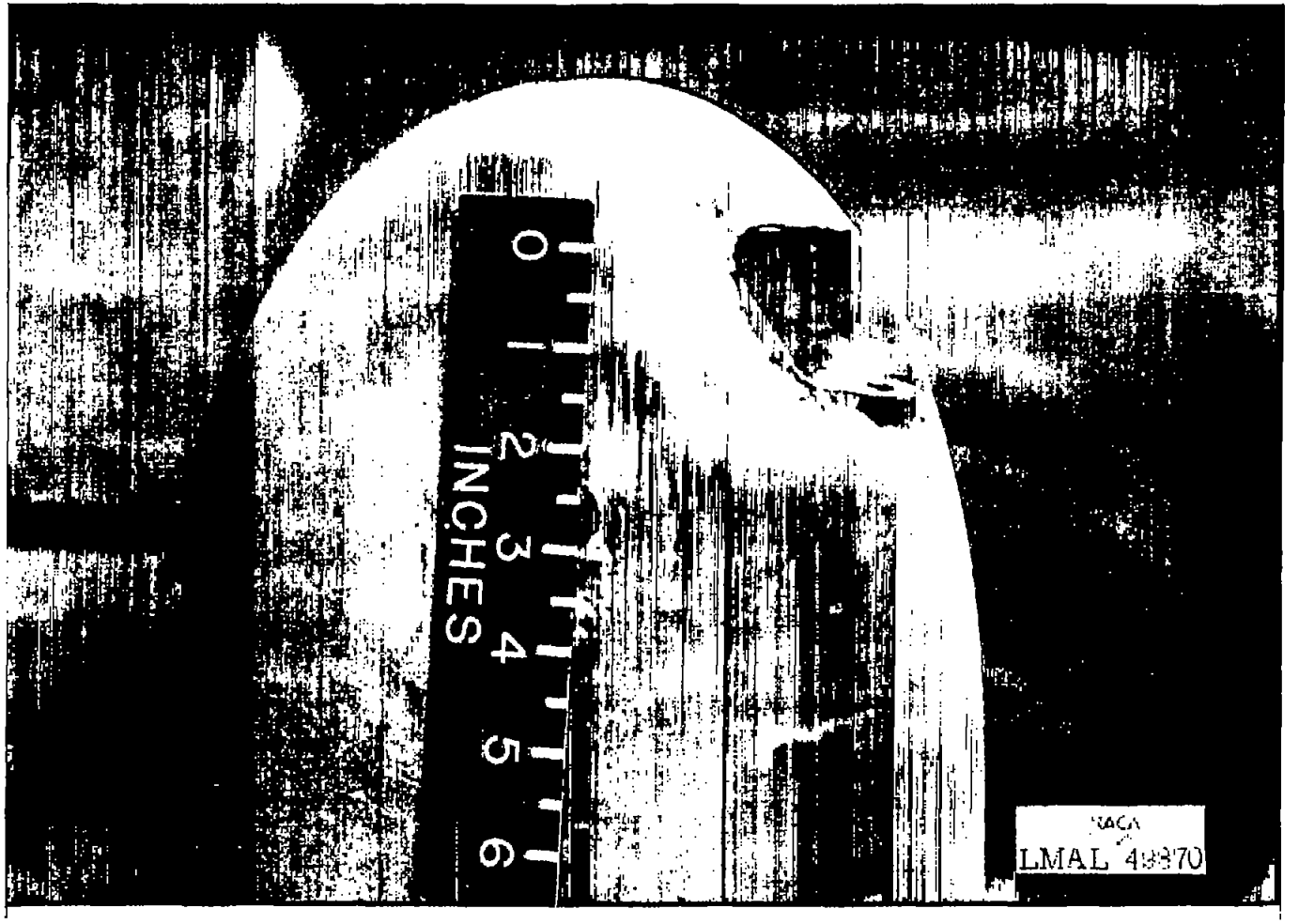

(a) Top view.

Figure 14.- Flow from revised blade-tip nozzle.

NATIONAL ADVISORY COMMITTEE FOR AERONAUTICS
LANGLEY MEMORIAL AERONAUTICAL LABORATORY - LANGLEY FIELD, VA

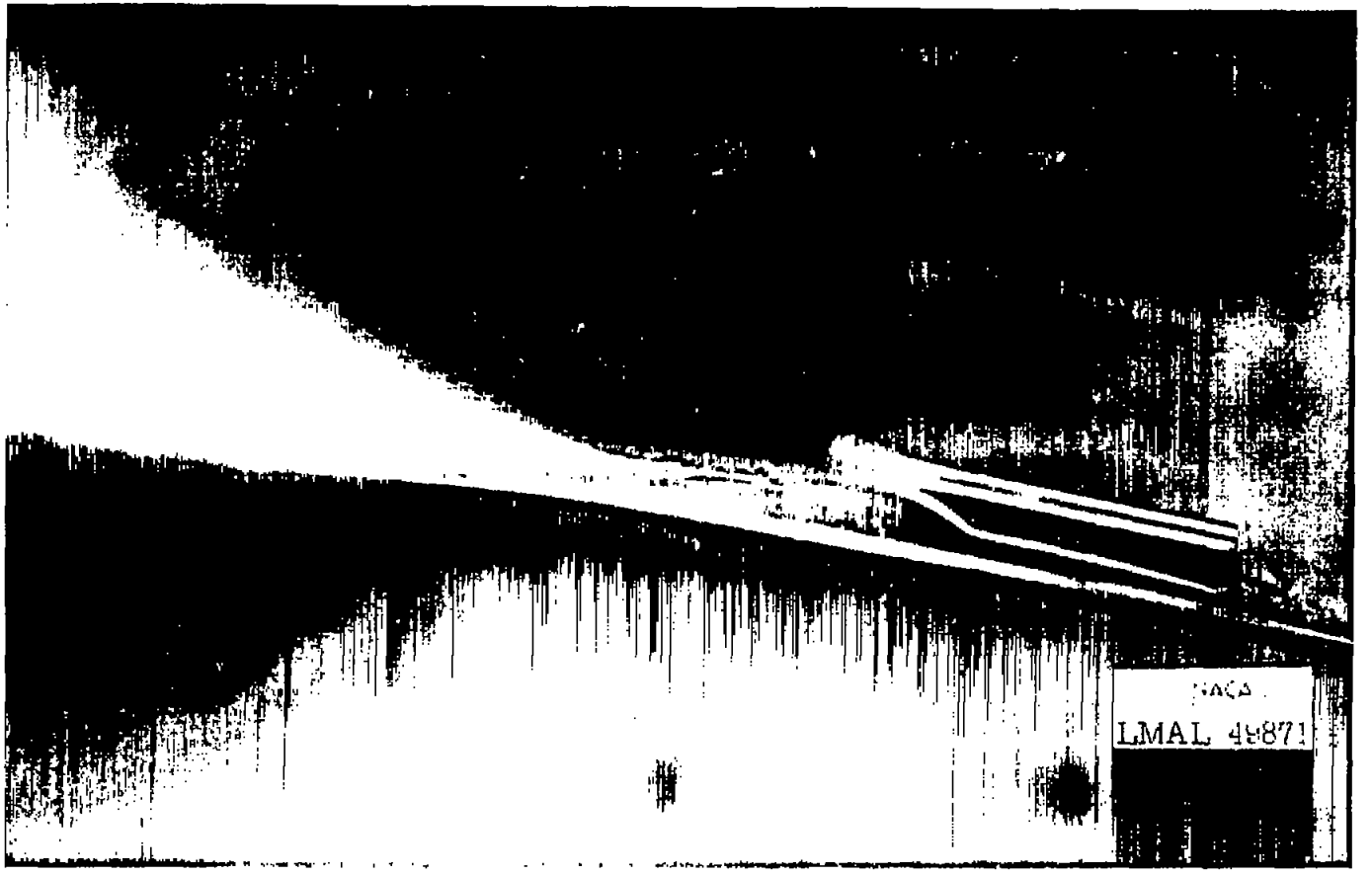

(b) End view.

Figure 14.- Concluded.

NATIONAL ADVISORY COMMITTEE FOR AERONAUTICS
LANGLEY MEMORIAL AERONAUTICAL LABORATORY - LANGLEY FIELD, VA

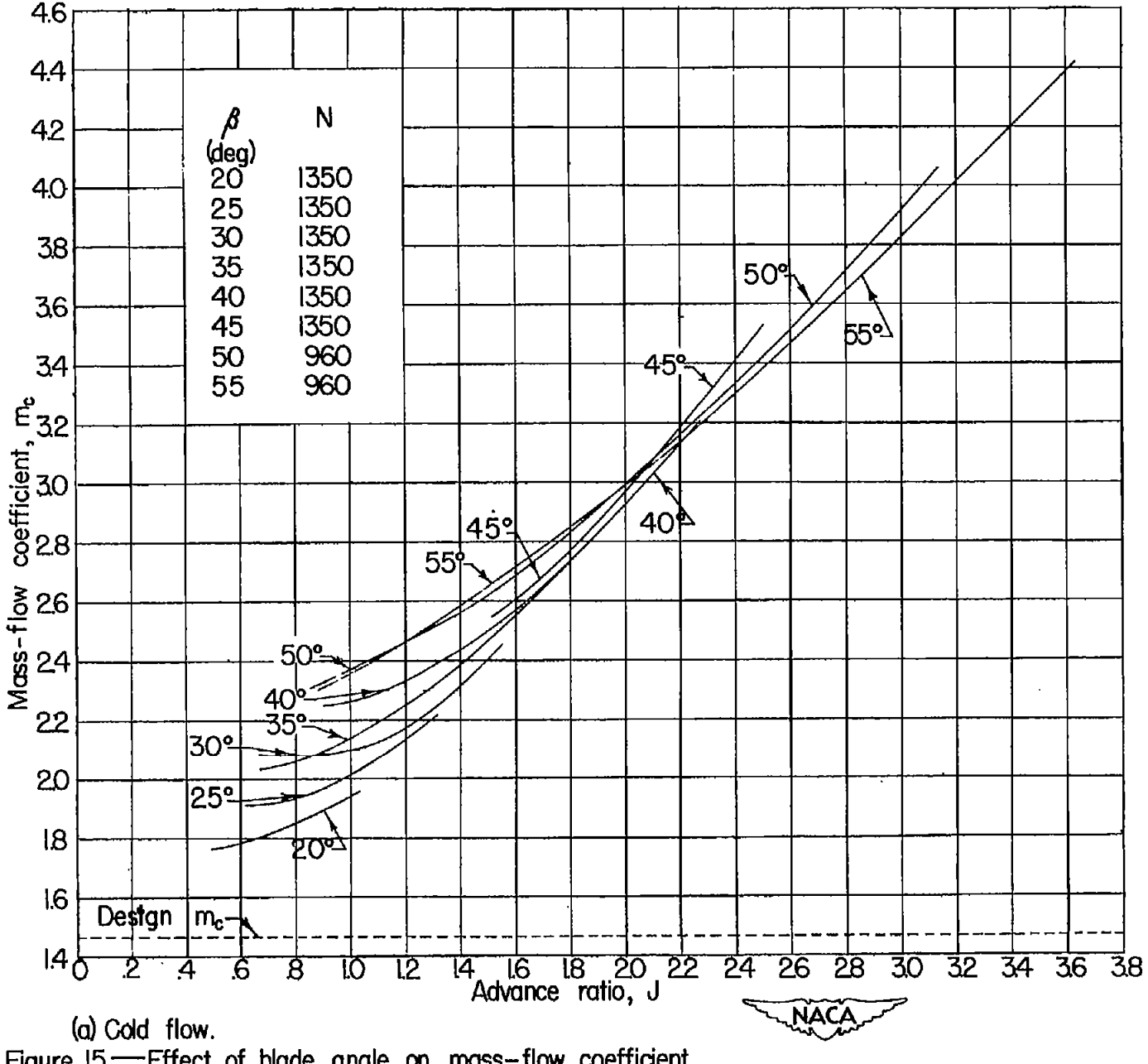

(a) Cold flow.

Figure 15.—Effect of blade angle on mass-flow coefficient.

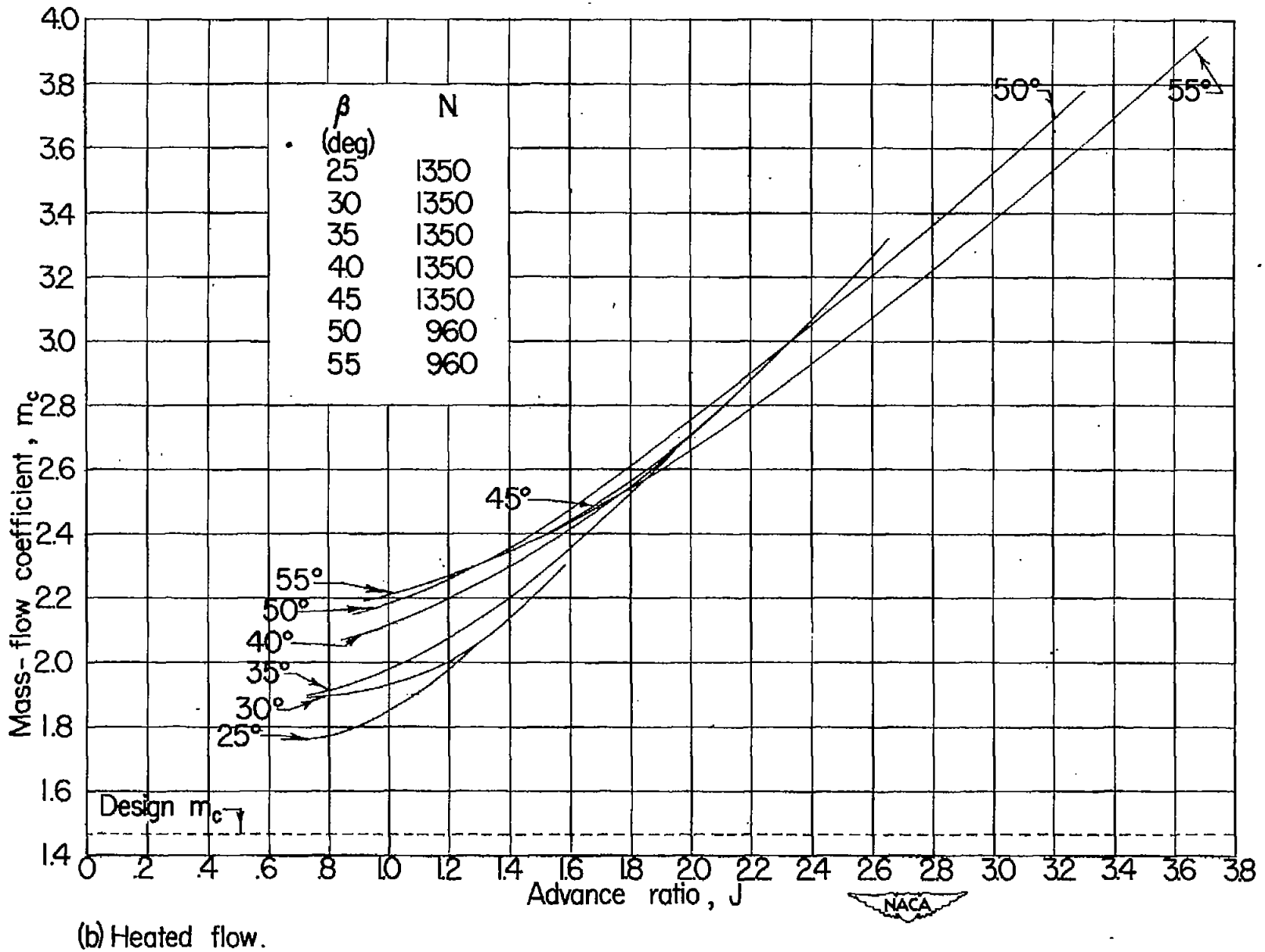

(b) Heated flow.

Figure 15.— Concluded.

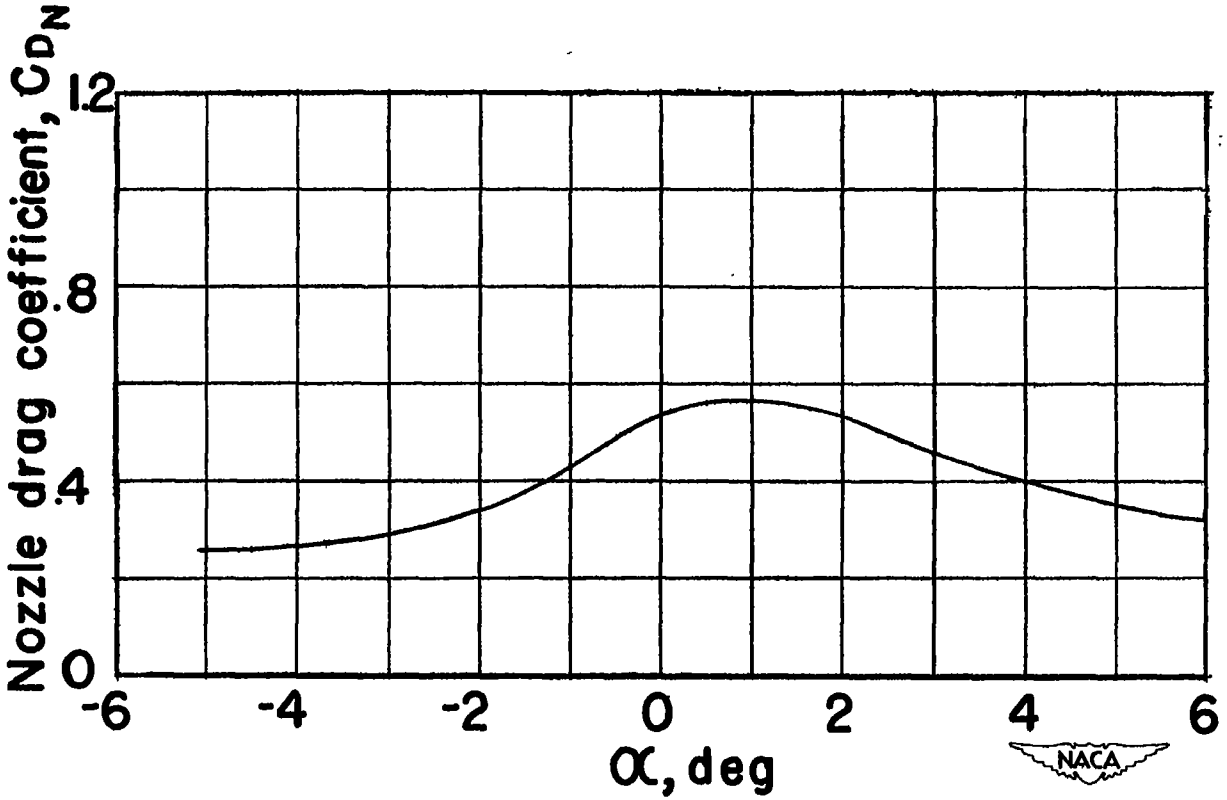

Figure 16.—Variation of nozzle drag coefficient with angle of attack.